SYNTHESIS OF POTASSIUM/SiO_2 CATALYST FROM LOCAL SOURCES AND TESTED BY TRANSESTERIFICATION OF CASTOR SEED OIL

BY

NNAMCHI, Anthony Chidi

MEng/SEET/2017/6696

DEPARTMENT OF CHEMICAL ENGINEERING

FEDERAL UNIVERSITY OF TECHNOLOGY

MINNA

OCTOBER, 2021

ABSTRACT

There is a need for the utilization of locally sourced heterogenous catalysts for biodiesel production to curb the challenges associated with homogeneous catalysts. The aim of this study was to produce an active catalyst from ripe plantain peels and rice husk for biodiesel production. Locally sourced caustic potash from ripe plantain peels doped with Rice Husk; a heterogeneous solid catalyst, was made by wet impregnation at totally different preparation conditions: calcination of the RH before doping with KOH and doping the RH with KOH before calcination labelled catalysts A and B respectively. The properties of the catalysts were determined utilizing Brunauer-Emmett-Teller, Scanning electron microscopy, X-Ray Diffraction, Energy Dispersive X-ray, and Fourier Transform-Infrared spectrum analysis. The Synthesised catalysts A and B were used for biodiesel production through Transesterification reaction of castor oil exploiting Response Surface Methodology, with three level-three factor randomised optimal design of temperature: 55^{o}C to 65^{o}C; catalyst loading: 2.0 to 3.0 wt/wt%; and time: 60 to 120 mins. The alcohol to oil proportion was kept constant at 6:1. Each of the catalysts showed chemical process activity, but catalyst B had a higher yield of 88.92 % biodiesel as compared to that of catalyst A of 77.76 % biodiesel. The kinetic study on the seed oil carried out at three different temperatures of 60, 61 and 62^{o}C, showed a pseudo first order rate constant and rate law with a very high activation energy of about 36.03 KJ/mol. The reusability study carried out on the oil sample for 4 consecutive runs under the optimum conditions showed a slight decrease on the yield from 88.92 to 86.15 as the reaction progressed from the 1st run to the 4th run. Hence, it could be concluded that locally sourced caustic potash doped with Rice Husk catalyst has very high catalytic activity and is better than caustic potash from plantain peels alone.

CHAPTER ONE

1.0 INTRODUCTION

1.1 Background to the Study

The use of energy has been considered the greatest essential requirement for human existence (Ling Zhou 2013). In the world's energy supply radar, petroleum constitutes the majority among other different kinds of fuels. Petroleum is found to play a significant role in industry, transportation, and agriculture, as well as to meet many other basic human needs (Saydut *et al*., 2016). Enormous increase in population size, increase in energy demand, exhaustion of fossil fuel reserves all conglomerate with the environmental problems associated with fossil fuel usage and these, in turn, have led to the search for different source of fuels which can be found in renewable sources (biofuel) (Ahmed *et al*., 2016). Biodiesel is a form of diesel fuel that is bio-degradable, renewable and environmentally favourable, that is derived from oils from vegetable or animal sources, that consists of long chain fatty acid esters. High capital and production cost, as mentioned by Amin and Amin (2015), have stood as the main impediment in the industrialization of biodiesel which has led researchers to focus on non-edible and waste oils (WO) as raw material to enhance biodiesel production.

Homogeneous base catalysts can change oils to their equivalent fatty acid methyl esters (FAMEs) with high produce, minimal time and cost efficiency but the process of renewing, separation of the catalyst from the product mixture and the environmental hazards during disposal poses some challenges in the use of these catalysts (Feng and

Zhen 2016). These challenges can be minimised or eliminated by the use of heterogeneous catalysts (Nasreen *et al*., 2018).

Potassium has been found to be the most plentiful mineral in plantain peels having given the value of $37gkg^{-1}$, by estimation, in the green peel. This estimated value has been proven to increase during the ripening stages by a small volume (Efeovbokhan *et al*., 2016). According to the results of the investigations carried out by several researchers concerning potash alkali and other metal constituents of the ashes found in plantain peels, it has been realised that the alkali component of the ash falls within the range of 69 to 81.9% with the analysed concentration of potassium in the peels giving values in excess of 750 mg/kg. According to Efeovbokhan *et al*., (2016), under the same process conditions of trans-esterification, KOH extract from ripe plantain peels ash gives higher percentage conversion than the commercial KOH.

Rice husk (RH) is a promising feedstock with very high abundance in nature and wide composition and these properties have given it a good edge for industrial applications. Just as other lignocellulosic materials, a typical rice husk houses cellulose, hemicellulose, lignin and ash (Touhami *et al.*, 2017). The striking surprise is that there are exceptional characteristics in the inclusion of high amount of silica in the rice husk, huge number of porous spaces in the rice husk, negligible weight of the rice husk and high distribution of surface areas exhibited by this biological waste (Soltani *et al.*, 2015). These properties have made rice husk a highly sort-after biological waste for typical adsorption process as a latent adsorbent, construction materials as a ligand, in the ceramics industry, a process accelerator or a support for other catalysts for other uses such as biodiesel production (Touhami *et al.*, 2017). The ash of rice husk, an agricultural waste, has been reported to contain silica (SiO_2) within the range of 92–95%. It boasts of a very high porosity with negligible weight and enormous surface area. There are several published journals with

the report of the use of rice husk ash as a support for other metal process accelerators (Thabet *et al.,* 2015).

1.2 Statement of the Research Problem

The necessity for efficient use of heterogeneous catalysts and/or renewable biomass resources has risen in recent years due to the challenges associated with homogeneous catalysts (Nasreen *et al*., 2018). The challenges imposed by homogeneous catalysts during biodiesel production includes non-reusability property, the high cost and unavailability of conventional resources, the difficulty of separating the catalysts after reaction, the high amount of wastes after reaction, and the air pollution leading to increased environmental concern imposed by homogeneous catalysts (Alueshima *et al*., 2018). Moreso, there is a need to conduct a kinetic study on the trans-esterification of *Ricinus communis* seed oil using the synthesised catalyst.

1.3 Justification of the Study

The use of homogenous catalysts and edible oils from vegetable sources in Transesterification has limited industrial production of biodiesel which has challenged the commercialisation of biodiesel. The option of locally sourced feedstock is an alternative to eliminate/limit the associated challenges because heterogeneous catalysts are renewable and there is little or no effort in separating heterogeneous catalysts from the product mixture for recycling. In the same vein, heterogeneous catalysts are reusable and the feedstocks are abundant and easily accessible in all parts of Nigeria.

1.4 Aim and Objectives of the Study

The research project is aimed at the synthesis of potassium/SiO_2 catalyst from local sources for the kinetic study of transesterification of castor (*Ricinus communis*) seed oil using methanol.

This aim shall be achieved through the following objectives:

1 Synthesis of plantain peels potassium hydroxide (KOH) doped on rice husk.

2 Characterisation of the synthesised catalysts using XRD, SEM/EDX, FT-IR and BET

3 Characterisation of *Ricinus communis* seed oil using standard method.

4 Kinetic study of biodiesel production using the catalyst prepared.

5 Determination of the characteristics of the biodiesel produced.

1.5 Scope of the Study

This research is only limited to the synthesis of potassium/SiO_2 catalyst from local sources for the kinetic study of transesterification of *Ricinus communis* seed oil with methanol and the characterisation of fatty acid methyl ester produced in terms of the ester analytical properties.

CHAPTER TWO

2.0 LITERATURE REVIEW

Over the years, researchers have been working tirelessly to find a different source of energy that can compete favourably with, if not replace entirely, conventional petrol (Marwaha *et al.,* 2018). Biodiesel an alternative to petrol fuel has attracted much attention because it has found its usefulness in conventional diesel engines due to the challenges of accessibility and the present rise in petroleum price (Ahmed *et al*., 2016).

According to Zahan *et al.* (2018), the history of sourcing an alternative fuel to petrol fuel started when Sir Rudolf Diesel successfully run, without any amendment, common diesel engines with vegetable oil in the nineties. Vegetable oil was utilised in the 1930s and 1940s, as engine fuel, mostly in the cases of utmost urgency.

Nevertheless, extra verification through investigation has it that it is unrealistic, the straight application of animal as well as oils from vegetable sources as engine fuel as a result of some of their properties like massive molecular mass, high kinematic viscosity, as well as low volatility. These properties decrease the engine efficiency and at same time pose other difficulties like sticking of the oil, thickening, gelling, and even engine knock. Several approaches such as blending with petro-diesel, micro-emulsification, thermal cracking otherwise known as pyrolysis, and transesterification have been put into practice in a bid to get the better of these difficulties and allow its application as a fuel (Marwaha *et al*., 2018).

2.1 Biodiesel Production Methods

As established by Dhikra *et al.,* (2018), the fact that biodiesel can be formed from many sources that are oil-based (edible and non-edible oils from vegetable sources, and animal fats) and the accrescent quest for a method to find enough quantity of biodiesel in a commercial scale have resulted in several production methods.

The biodiesel production methods include pyrolysis, micro-emulsification, blending and transesterification (Nisar *et al*., 2017; Marwaha *et al*., 2018).

2.1.1 Pyrolysis (thermal cracking)

Pyrolysis alludes to a chemical transformation brought about by the utilisation of thermal energy in the nonattendance of air/oxygen, or by the application of heat within the sight of a process accelerator, which brings about cleavage of bonds and formation of an assortment of small molecules. Pyrolysis is directed at temperature extend of 400–600 ℃ (Gebremariam & Marchetti, 2017).

The common oils for the pyrolysis technique for the biodiesel production can extend to oils obtained from vegetables, fats from animals, common unsaturated fats and/or methyl esters of unsaturated fats (Mishra & Goswami, 2017).

It has been seen, according to Nisar *et al* (2017), that the chemical transformation of triglycerides to get biodiesel is appropriate for diesel engines. The liquid portions of the temperature-dependent transformation of oils from vegetables are probably going to move towards fuels of diesel. This kind of disintegration of oils gives rise to aromatics, alkadienes, alkenes, alkanes, and carboxylic acids

Mishra and Goswami (2017), additionally stated that biodiesel fuel obtained through a pyrolysis procedure otherwise known as bio-oil is appropriate for diesel motors; be that

as it may, low-worth materials are created because of the exclusion of oxygen during the process.

Another impediment of pyrolysis is the requirement for refining hardware for separation of the different fractions. Likewise, the bio-oil produced is like petrol containing sulphur which makes it less eco-friendly (Gebremariam & Marchetti, 2017).

The hardware for pyrolysis is costly for humble production of biodiesel. Similarly, while the bio-oils are similar to fossil-generated petrol and diesel fuel, the expulsion of oxygen during the thermal processing additionally evacuates any natural advantages of utilising an oxygenated fuel. It creates some low worth materials and, at times, more gas than diesel fuel (Gashaw *et al.*, 2015).

2.1.2 Micro emulsification

Microemulsion creation is, latently, an answer to the issue of thickness of vegetable oil. Microemulsion is proven to be straightforward, a colloidal scattering that is thermodynamically steady. Microemulsion, a colloidal balance scattering of optically isotropous liquid of microstructure (with measurements for the most part 1 to150 nano meters) that possess extemporaneous shapes found in 2 typically non-miscible fluids with at least 1 ionic amphiphiles (Gashaw *et al.*, 2015).

The formation of microemulsions can be by utilisation of strippers such as 1-butanol, ethanol, hexanol, methanol and butanol. Microemulsions formed from these strippers conform with the most extreme thickness necessities for diesel fuel. The created of microemulsions is initialised with oils from vegetables, an ester and a co-solvent (dispersant), or oils from vegetables, liquor, surface-active agent and cetane reformer inclusive or not of diesel oil (Gebremariam & Marchetti, 2017).

When microemulsions are created with anyone of hexanol, octanol or butanol, they mostly meet the most extreme viscosity prerequisite for diesel oils (Nisar *et al.,* 2017).

The 2-octanol was seen as an effective amphiphile in the micellar solubilisation of methanol in triolein and soybean oil. When microemulsions are created with anyone of hexanol, octanol or butanol, they mostly meet the most extreme viscosity prerequisite for diesel oils known as Number two diesel (Mishra & Goswami, 2017).

2.1.3 Blending

It was recommended in nineteen eighties that oils from vegetative could be utilised as diesel oils. The idea of utilising consumable triglyceride in place of fuel implied oil would be exchanging fuel as opposed to oils from vegetable sources and liquor as the other options and other type of sustainable power sources to replace non-inexhaustible assets (Nisar *et al.*, 2017).

In 1980 at Brazil, a blend of 10% oils from vegetable sources were used to run pre-burning chamber motors to keep up all out force with no modifications or changes in accordance with the motor in Caterpillar. By then, it was not a pragmatic step, subbing 100% oils from vegetable sources with diesel oils, yet, it was reasonable, a mix of 2:8 oils from vegetable-to-diesel oil and it worked (Gashaw *et al.*, 2015).

Unadulterated oils from vegetable sources as well as blends have commonly been considered unsuitable, illogical and difficult both for direct and indirect diesel motors. It has been noticed and seen that there are evident issues developed as a result of viscosity in its high values, composition of the acid, free fatty acid content and development of gum because of corrosion and polymerisation during capacity and burning, carbon build-ups and greasing up oil thickening (Gebremariam & Marchetti, 2017).

2.1.4 Transesterification

The most widely recognized approach to yield FAME is the transesterification technique, which alludes to a catalysed synthetic reaction including vegetable oil and liquor to biodiesel and glycerol (Mishra & Goswami, 2017). The reaction needs a process accelerator, normally a strong base, for example, sodium and potassium hydroxide or sodium methylate and/or sulphuric acid-based transesterification processes (Zahan & Kano, 2018). Acid catalysts are too delayed to possibly convert triglycerides to biodiesel (Mishra & Goswami, 2017); be that as it may, acid catalysts are very viable at converting FFAs to biodiesel (Nisar *et al.*, 2017). Along these lines, an acid catalysed pre-treatment venture to convert the FFAs to esters, succeeded by an alkali-catalysed venture to convert the triglycerides ought to give a productive technique to convert high FFAs to biodiesel. According to Gebremariam and Marchetti (2017), transesterification process decreases the viscosity of the oil and a catalyst is generally used to improve the reaction rate and the conversion. As reported by Zahan & Kano, (2018), since the reaction is reversible, overabundance alcohol is utilised to move the balance to the product side. Particularly methanol is utilised as liquor on account of its cost effectiveness and its physical and chemical favourable qualities. Methanol can rapidly react with vegetable oil and NaOH can undoubtedly dissolve in it (Mishra & Goswami, 2017). The stoichiometric response requires 1 mol of a triglyceride and 3 mol of the liquor. Nonetheless, an overabundance of the liquor is utilised to build the yields of the alkyl esters and to permit its phase separation from the glycerol formed. The triglycerides are reacted with an appropriate liquor (Methyl, Ethyl, or others) within the sight of a catalyst under a controlled temperature for a given period of time (Zahan & Kano, 2018).

Table 2.1: Summary of different methods of transesterification processes, their merits and demerits (Gebremariam & Marchetti, 2017; Zahan & Kano, 2018; Nisar *et al*., 2017; Mishra & Goswami, 2017)

Methods	Type of feedstock	Merits	Demerits
Homogeneous Acid catalysis	Oils of any kind, high and low free fatty acid content inclusive	i. High biodiesel yield. ii. Not affected by FFA content, hence, accepts low-grade oils. iii. Energy requirement is quite minimal. iv. Both esterification and transesterification reactions happen in a step.	i. High amount of glycerol in the product. ii. Operates with high temperatures. iii. Longer reaction time. iv. Difficulty separating catalyst from product. v. Acid corrosiveness affects equipment.
Homogeneous Base catalysis	Oils with low free fatty acid content (max FFA of 0.5%wt oil)	i. Mild reaction condition with minimal energy requirement. ii. Rate of reaction higher than homogeneous acid catalysed transesterification. iii. Common catalysts are cheap and readily available. iv. Less corrosive	i. Affected by the oil FFA content. ii. High tendency of soap formation. iii. Difficulty in glycerol recovery. iv. Cost of treatment of alkaline water generated.
Heterogeneous Acid catalysis	Oils of any kind, high and low free fatty acid content inclusive	i. Easy separating catalyst from product. ii. Both esterification and transesterification reactions happen in a step. iii. Reusability of catalysts. iv. Perfect with low grade oils. v. Minimal process stages and wastes. vi. Insensitive to oil FFA content.	i. High cost of catalyst synthesis. ii. Operates with high temperatures. iii. Longer reaction time. iv. High molar ratio of alcohol to oil v. Energy requirement is relatively high
Heterogeneous Base catalysis	Oils with low free fatty acid content (max FFA of 0.5%wt oil)	i. Mild reaction condition with minimal energy requirement. ii. Easy separating catalyst from product. iii. Reusability of catalysts. iv. Minimal process stages and wastes. v. Improved selectivity.	i. High tendency of soap formation. ii. Sensitive to oil FFA content. iii. Difficulty in product purification. iv. Contamination of product due to leaching of active sites. v. Easily affected on exposure to ambient air.

Table 2.1 – Continuation.

Methods	Type of feedstock	Merits	Demerits
Nano catalysed transesterification	Oils of any kind, high and low free fatty acid content inclusive	i. High rate of reaction. ii. Minimal amount of catalyst. iii. Reusability of catalyst. iv. Varieties of catalysts available.	i. Increased amount of alcohol required. ii. High cost of catalyst preparation.
Ionic liquid catalysed transesterification	Oils of any kind, high and low free fatty acid content inclusive but depends on which type of ionic liquid used (Acidic/Basic).	i. Ease of product separation. ii. Flexibility of catalyst properties during synthesis. iii. Reusability of catalyst and ease of separation. iv. Time saving and efficiency of process. v. High catalytic activity and stability.	i. Increased amount of alcohol required. ii. High cost of catalyst preparation
Lipase catalysed transesterification	Oils of any kind, high and low free fatty acid and water contents inclusive	i. Easy separating catalyst from product. ii. Operates under low temperatures. iii. Reusability of immobilized enzymes. iv. Perfect with low grade oils. v. Ease of purification with simple steps. vi. High purity ester is produced. vii. Insensitive to oil FFA and water contents.	i. High cost of enzymes. ii. Low reaction rate. iii. Lipase inactivation caused by methanol and glycerol.
Supercritical transesterification	Oils of any kind, high and low free fatty acid & water contents inclusive	i. Minimal reaction time. ii. Gives very high ester yield. iii. Doesn't required further purification process. iv. A continuous process. v. Not affected by FFA or water content of oil.	i. High temperature and pressure. ii. Economically not viable. iii. High methanol consumption.

Table 2.2: Summary of biodiesel production methods (Zahan & Kano, 2018; Nisar *et al*., 2017)

Methods	Main Process	Advantages	Disadvantages
Pyrolysis (thermal cracking)	Oils from vegetable and/or animal sources are warmed and decayed at raised temperature above 350 ^{o}C regardless of the availability of the process accelerator. Analysis of various liquid or gaseous items conditioned on boiling points to ascertain the specific item.	It is an efficient process, straightforward (doesn't need to be washed, dried or sifting), doesn't contain wastes, contamination free.	Required high temperature and costly equipment and produce low immaculateness of biodiesel (contain heterogeneous atoms including ash and cokes).
Micro-emulsification	Oils from vegetable and/or animal sources were made soluble with a surface-active agent and liquor and till the necessary viscosity was attained.	Simple procedure as well as contamination free at the same time.	High viscosity, low stability (the inclusion of ethanol can improve the amount/quality of surfactant required to keep up the condition of microemulsion), and could prompt sticking, incomplete combustion, and coking.
Blending (dilution)	Preheated vegetable/animal oils were mixed with petro-diesel in a 10–40% (w/w) proportion. Then the resulting oil-diesel blend was applied on a diesel engine.	Doesn't need chemical procedures (non-contaminating), nonattendance of practical adjustments, and simple operation.	High viscosity, instability, low explosiveness, as well as increment in percentage of oils from vegetable/animal brought about inappropriate spraying design, poor atomization, inadequate fuel ignition, and trouble in dealing with, by customary motors.
Transesterification	Oils from vegetable and/or animal sources and fats were reacted with liquor (ethanol or methanol) in the presence of a process accelerator (alkali or acid). The by-product and the biodiesl will be separated and decontaminated and then utilised.	High yield with comparatively minimal cost, mild reaction conditions, properties in conformity with that of conventional diesel and can be applied for large-scale production and commercialisation	Low FFA as well as moisture contents in the crude material are needed, broad separation and decontamination steps, potentials for side reactions and large volume of wastewater generation when homogeneous catalysis is involved.

2.2 Effect of Process Parameters on Biodiesel Yield

Table 2.3: Summary of the effect of process parameters on biodiesel yield

Parameters	Properties	References
Free Fatty Acid (FFA) and Moisture contents	The Free Fatty Acid and moisture content of an oil is very important parameter that determines the quality and applicability of the oil. These properties affect transesterification reaction negatively as their presence in the oil above the required level causes saponification reaction, hence, a low biodiesel yield. FFA content is advised to be <1%.	Mishra & Goswami, 2017
Catalyst Loading	The catalysts employed for transesterification reaction are acid, base or enzyme catalysts. Studies have shown that ester conversion is dependent on catalyst loading. An increased catalyst loading, to the optimum amount, increases ester yield but an excess catalyst amount will react with the oil, causing an emulsion formation which increases the viscosity of the reactants and in turn, further result to a low ester yield and difficulty in the separation of the final product.	Mishra & Goswami, 2017; Oladipo *et al.*, 2018; Maniam, *et al.*, 2015; Dhikrah, *et al.*, 2018.
Alcohol to Oil Molar ratio	A stoichiometric molar ratio of alcohol to oil for transesterification reaction is established to be 3:1 but studies have shown that the solubility and the contact between the alcohol and the triglyceride molecules are enhanced with higher molar ratios, hence, ester conversion is enhanced as well. Report showed that the yield of ester does not increase proportionally with alcohol-to-oil molar ratios and that higher ratio in favour of alcohol results in an apparent decrease in ester conversion which in turn hinders glycerol separation because alcohol with one polar hydroxyl group can pose as an emulsifier when used in excess.	Mishra & Goswami, 2017; Maniam, *et al.*, 2015; Dhikrah, *et al.*, 2018; Oladipo *et al.*, 2018.
Reaction time	Reaction duration is another important parameter in biodiesel production. Research showed that an increase in reaction time favours ester formation until the equilibrium is reached when the ester yield would appear to be constant. Further increase in reaction duration above the optimum time results in retarded ester yield. This is reported to be as a result of the reversibility of the reaction and this poses difficulty in product separation.	Oladipo *et al.*, 2018; Mishra & Goswami, 2017; Maniam, *et al.*, 2015; Dhikrah, *et al.*, 2018.
Temperature	The temperature of reaction is a very important factor that enhances ester conversion. Thermal energy is highly needed to overcome diffusion resistance between different reactant phases (methanol-oil-catalyst). Ester yield is favoured by an appropriate increase in the reaction temperature. Further increase in reaction temperature above the alcohol boiling point will vapourise the alcohol making it form bubbles which inhibits any reaction on a two-phase interface, hence, a decrease in biodiesel yield.	Mishra & Goswami, 2017; Maniam, *et al.*, 2015; Dhikrah, *et al.*, 2018.

2.3 Typical Oils used in Biodiesel Production

Table 2.4: Different oil sources for biodiesel production (Mujeeb *et al*., 2016)

Group	Oil Sources
Inedible oils	Babassu tree, copaiba balsam, honge, jatropha or ratanjyote, jojoba, karanja or honge, mahua, milk bush, nagchampa, neem, petroleum nut, rubber-seed tree, silk-cotton tree, and tall, recinus cumnis.
Major oils	coconut, corn, cotton-seed, rapeseed, olive, ground-nut, false saffron, sunflower, soy-bean, and sesame
Nut oils	Almond, cashew-nut, hazel-nut, macadamia, pecan, pistachio and wal-nut
Other edible oils	Amaranth, apricot, argan, artichoke, avocado, babassu, bay laurel, beech-nut, ben, Borneo tallow-nut, carob pod (algaroba), cohune, coriander seed, false flax, grape seed, hemp, kapok seed, lallemantia, lemon seed, macauba fruit (*Acrocomia sclerocarpa*), meadowfoam seed, mustard, okra seed (hibiscus seed), perilla seed, pequi, (*Caryocar brasiliensis* seed), pine-nut, poppy seed, prune kernel, quinoa, ramtil (*Guizotia abyssinica* seed or Niger pea), rice bran,tallow, tea (camellia), thistle (*Silybum marianum* seed), and wheat germ

2.4 Raw Materials used for the Study

2.4.1 Castor seed oil

Non-edible oils from vegetable sources have been the most widely accepted feedstocks for biodiesel production and castor seed oil has become one of the highly regarded of them all because of its fascinating spectacles (Keera *et al.,* 2018). These interesting phenomena exhibited by castor seed oil as a biodiesel raw material are two and they include:

a) Castor seed oil poses no competition with edible oils from vegetable sources;

b) Castor seed oil can be cultivated with ease.

According to Keera *et al*., (2018), the oil extracted from the castor seeds are widely known to contain a very high oil content of about 40–55% which is very high when

compared to most other commonly used non-edible oil crops such as soybean (15–20%), sunflower (25–35%), and rapeseed (38–46%).

More so, castor oil has a composition which leaves it at a disadvantage as a source of oil for FAME invention as it is comprised mostly of hydroxyl fatty acid (about 90%), ricinoleic acid and non-hydroxylated fatty acids (about 10%), mainly oleic and linoleic acids. This fact is the reason for its high viscosity which is 7 times above any other oils from vegetable sources' viscosity (Yusuf *et al*., 2015; Panhwar *et al*., 2016; Beruk *et al*., 2018; Keera *et al.,* 2018). As reported by Yusuf *et al*., (2015), it can be said that castor seed oil is a very unique non-edible oil that has a very high quantity of fatty acid that cannot be compared with any other non-edible oil. Yusuf et al reported that castor seed oil contains low quantity of saturated and polyunsaturated fatty acids which is a revelation of its fatty acid profile. The above facts enhance castor seed oil's stability.

Castor seed oil, just like other oils from vegetable sources, vary in composition and properties and this is due to the disparity in the extraction method, location, and the cultivar type. Castor seed oil, macadamia nut, olive, palm kernel and sunflower oil share the same fatty acid profile (Yeboah *et al.,* 2020).

In ricinoleic acid of the castor oil molecule, there exists a hydroxyl group (–OH) attached to the hydrocarbon chain, and these property makes castor oil chemically unique from any other non-edible oil. Another intriguing property is its raised viscosity and polarity which render castor seed oil tremendously valuable for the industries (Keera *et al.,* 2018). However, castor seed oil is very useful in numerous subdivisions such as agricultural, pharmaceutical, and industrial sectors. Castor seed oil can be used to produce: ointments, nylon, varnishes, airplane engine lubricants, hydraulic fluids, dyes, detergents, plastics, coatings, synthetic leather, cosmetics, and perfumes (Keera *et al.,* 2018; Ying et al., 2017;

Yeboah *et al.*, 2020). It also upsurges the lubricity when compared to usual oils from vegetable sources and becomes effective as additive for diesel fuel. This same property has resulted in a better oxidation stability and lowered melting point of castor seed oil by increasing its solubility in alcohol which also a measure of its readiness to easily be converted to biodiesel at lower temperatures. Castor oil has excellent ability to withstand low temperatures brought about by the high amount of unsaturated fatty acid (Keera *et al.*, 2018).

Castor seed oil is an oil extract from an annual oil seed crop commonly called castor with a botanical name of *Ricinus communis* (Yeboah *et al.*, 2020). Castor shrub has some seeds and is sometimes referred to as castor bean even though it is not a true bean in nature. This shrub can grow in different geographical areas and it belongs to the spurge family called Euphorbiaceae. Castor can thrive in areas with temperature within the range of 12^{o}C and 38^{o}C. Any temperatures above or below this range cannot favour castor germination and yield. According to Sbihi *et al*., (2018) There is a tremendous disparity in growth, appearance, growth pattern, seed colour, seed size, stem colour, foliage and oil content of castor shrubs. Castor seed can be either elongated, ovoid, oval, or square in shape. Its size varies from 0.5 to 1.5 cm long. The seed is comprised of many colours (a colour varying from brown to black or red to black for the base, brownish yellow, grey, and white). It has patterns, as reported by Naik (2018), ranging from fine-to-coarse vein-like or finely dotted splotches to broad splotches. As reported by Sbihi *et al*., (2018), the leaves change based on the content of anthocyanin pigmentation and it changes from pale green to dark red. The fruit has a globe-like shape similar to a spiny capsule and the capsule in which the seeds are enclosed in cracks when the fruit fully matures (Yeboah *et al.*, 2020).

Gad-Elkareem *et al*., (2019), stated that castor oil production is presently higher in areas such as India, China, and Brazil. The seed oil content percentage of castor plant ranges from 40 to 60% and its annual oil production records about 1.8 million tons globally. The understanding of castor oil is constructed on the ricinoleic acid structure, carboxylic group, hydroxyl group, and the single point of unsaturation (Yusuf *et al*., 2015; Mubofu, 2016). An extra strength is provided by these features to the structure of the oil.

2.4.2 Plantain peels

Plantain, a common staple food, abundant in West Africa with botanical name Musa paradisiaca is commonly eaten either boiled, fried, roasted, or baked. Plantain fruits can be consumed ripe or unripe but ripe plantains are higher in the preferential radar than the unripe ones (Etim *et al*., 2018). Africa generates about 64.22% of the World's plantain production of which about 7.7% comes from Nigeria. According to Olabanji *et al*., (2012), Nigeria's plantain fruits are not in the international market, in-spite of the large quantity produced yearly, rather it is largely consumed by the local populace. By records, there is a surge in home industries in the urban areas and these industries utilise snacks made from plantains like plantain chips. More so, the demand for locally made stress-free and opportune foods from plantain also helped increase plantain consumption (Olabanji *et al*., 2012).

The World plantain production in 2019 was about 41.58 million metric tons and Nigeria's share of the production was about 3.18 million metric tons (FAOSTAT, 2019). In Nigeria and West Africa at large, plantain fruits are consumed in great quantities and this high consumption rate gives yield to large quantity of plantain peels which are solid wastes and these waste materials are mostly discarded with few fractions used as animal feeds (Etim *et al*., 2018; Olabanji *et al*., 2012). It was reported that plantain peels can be utilised

in the production of ethanol, alkali for soap production and/or catalyst for biodiesel production and other medicinal use (Olabanji *et al*., 2012).

According to Usman *et al*., (2018), alkali synthesised from biological materials are often referred to as Bio-alkali(s). There is a large quantity of mineral salts that every agricultural material contains and it has been reported that when such materials are subjected to an open burning, contents like fats, vitamins, carbohydrates, and proteins will evaporate thereby leaving the ashes which will comprise the oxides of the constituent minerals. These oxides are predominantly oxides of sodium and potassium which will produce hydroxides of these elements when the respective ash is dissolved in water.

It has been established by research that the basic component from plantain peel ash has enormously been utilised in soap production, biodiesel production and lubricating grease of good quality. Hereafter, there is a growing forecast that the base from the ash of unwanted agricultural materials shall serve as renewable catalyst for transesterification (Usman *et al*., 2018).

In this study, the potassium hydroxide (KOH) used was derived from a renewable unwanted agricultural content in ripe plantain peels ash obtained from biomass resources (Efeovbokhan *et al*., 2017).

2.4.3 Rice husk

The attention of industries all over the world have recently shifted to the utilisation of unwanted agricultural residues as raw materials for their industrial productions and this comes as a result of such advantages as the cost effectiveness of the unwanted materials, their deficiency in competitiveness with food stream, the shift from the reliance on unrenewable material sources and their possible reduction in greenhouse gas emissions. There has been discovery of several unwanted agricultural materials like rice husk (RH),

sugarcane bagasse, coconut husk, rice straw, wheat straw, etc (Touhami *et al.*, 2017). In several parts of the world, RH has been noticed to be a great source of agricultural spin-off. The World rice production in 2019 was about 755.47 million metric tons; Africa recorded rice production of about 38.77 million metric tons and Nigeria's share of the production was about 8.44 million metric tons. Asia alone recorded rice production in excess of 677.28 million metric tons in 2019 (FAOSTAT, 2019).

The very high abundance in nature and wide composition properties of rice husk (RH), a promising feedstock, gives it a good edge for industrial applications. Just as other lignocellulosic materials, a typical rice husk contains cellulose, hemicellulose, lignin and ash (Touhami *et al*., 2017). The striking surprise is that there are exceptional characteristics in the inclusion of high amount of silica in the rice husk, large amount of porous spaces in the rice husk, negligible weight of the rice husk and high distribution of surface areas exhibited by this biological waste (Soltani *et al*., 2015). These properties have made rice husk a highly sort-after biological waste for typical adsorption process as a latent adsorbent, construction materials as a ligand, in the ceramics industry, a process accelerator or a support for other catalysts for other uses such as biodiesel production (Touhami *et al*., 2017; Chen *et al.*, 2013). Rice husk, an agricultural waste, has been reported to contain silica (SiO_2) in the ash (within the range of 92 to 95%). It boasts of a very high porosity with negligible weight and enormous surface area. There are several published journals with the report of the use of rice husk ash as a support for other metal process accelerators (Thabet *et al.*, 2015). Chandrasekhar *et al.,* (2006) reported that calcination temperature and heating rate have a great influence on the optical and catalytic properties of rice husk ash.

2.5 Kinetics of Transesterification Reaction

2.5.1 Model for trans-esterification reaction in a batch reactor

Transesterification reaction is a reaction between a triglyceride and alcohol in the presence of a catalyst to produce a mixture of fatty esters and glycerol as shown by the reaction equation below:

(a)

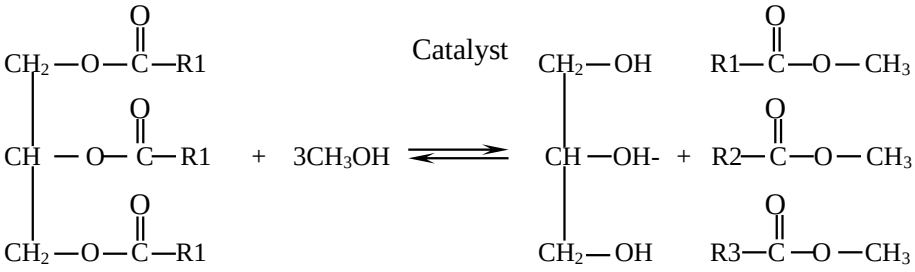

Source: (Amin and Amin 2015)

(2.1)

(b)

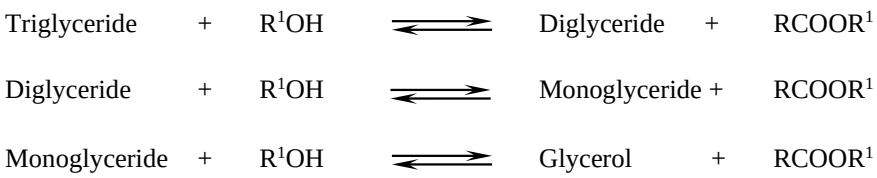

Source: (Adokiye *et al*., 2020)

As witnessed in the equation (2.1) which happens to be the equation of reaction, it is assumed that the reaction is a pseudo-first order reaction. This is because, being it that it is an equilibrium reaction, there is a need for an excess alcohol (an amount far greater than the stoichiometric quantity) so the reaction can favour forward reaction or in order to guarantee the production of biodiesel. Practically, alcohol in excess of 6 moles or more is utilised (Efeovbokhan *et al.*, 2017).

To determine the kinetics, we assume A to be the castor seed triglyceride (the reactant) whereas D is assumed to be the fatty acid methyl ester.

Hence, the reaction equation can be given by equation (2.2) as below:

$$A \rightarrow D \tag{2.2}$$

This produces the unvarying volume density of A in the reactor within the period, t.

Therefore, reactant design attributed to the batch reactor is:

$$\frac{dN_A}{dt} = -r_A V \tag{2.3}$$

N_A = amount of the reactant A for the period, t in the reactor.

r_A = reaction rate for A.

Expressing Equation (2.3) in terms of *X* (conversion), we have;

$$X_A = \frac{N_{AO} - N_A}{N_{AO}} \tag{2.4}$$

Re-arranging equation (2.4) gives

$$N_{AO}X_A = N_{AO} - N_A \tag{2.5}$$

$$\therefore N_A = N_{AO} - N_{AO}X_A \tag{2.6}$$

The differential form of equation (2.6) is

$$\frac{dN_A}{dt} = \frac{-N_{AO}dX_A}{dt} \tag{2.7}$$

Equating "equations (2.3) and (2.7)" results to

$$\frac{dN_A}{dt} = \frac{-N_{AO}dX_A}{dt} = -r_A V \tag{2.8}$$

Separating variables will result to (2.9) as thus:

$$dt = \frac{-N_{AO}dX_A}{-r_A V} \tag{2.9}$$

Applying the following conditions at the boundary and integrating; at t = 0, $X_A = 0$ and $at\ t = t_f$, $X_A = X_{Af}$.

$$\int_{t=0}^{t=t_f} dt = \int_0^{X_{Af}} \frac{N_{AO}dX_A}{(r_A)V} \Rightarrow t_f = \int_0^{X_{Af}} \frac{N_{AO}}{(r_A)V} dX_A \tag{2.10}$$

The final conversion of A is X_{Af}

The rate of disappearance of A, r_A has to be put as a function of X_A just to successfully carried out integration on equation (2.10) with an assumption that the volume V is constant.

But from the reaction equation, Equation (2.2), the rate at which A disappears or is converted to product can be expressed mathematically thus;

$$-r_A = K_1 C_A \tag{2.11}$$

K_1 = rate constant for the pseudo 1st order reaction and

$$C_{A=} \frac{N_A}{V} \tag{2.12}$$

The combination of equations (2.11) and (2.12) produces

$$-r_{A=} K_1 \frac{N_A}{V} \quad \Rightarrow \; -r_A V \; = \; K_1 N_A \tag{2.13}$$

A substitution of Equations (2.13) with (2.6) into Equation (2.8) yielded;

$$\frac{-N_{AO} dX_A}{dt} = \; K_1 (N_{AO} - \; N_{AO} X_A) \Rightarrow K_1 N_{AO} (1 - X_A) \tag{2.14}$$

Further simplification will give,

$$dt = \; \frac{-N_{AO}}{K_1 N_{AO} (1 - X_A)} dX_A \tag{2.15}$$

Applying the following conditions at the boundary and integrating; at t = 0, X_A = 0 and $at\ t = t_f$, $X_A = X_{Af}$

$$\int_0^{t_f} dt = \; \int_0^{X_{Af}} \frac{N_{AO}}{-K_1 N_{AO} (1 - X_A)} dX_A \; \Rightarrow \; \int_0^{X_{Af}} \frac{1}{-K_1 (1 - X_A)} dX_A \tag{2.16}$$

This means that;

$$t_f = \; -\frac{1}{K_1} \ln(1 - \; X_{Af}) \tag{2.17}$$

Where t_f is the time used for the transesterification reaction,

X_{Af} = the conversion at the reaction period, t.

Plotting a graph of t_f vs $\ln(1 - \; X_{Af})$ shall yield a straight-line graph with its slope as $-\frac{1}{K_1}$

2.5.2 Activation energy determination

The Arrhenius equation was employed to calculate the activation energy of the transesterification reaction by comparing the influence of temperature on the global reaction rate constant (Sarve *et al*., 2015). This was achieved by fitting *k* values into the Arrhenius equation,

$$k(\mathrm{T}) = k = \mathrm{A}.\, \mathrm{e}^{(-E_a/RT)} \tag{2.18}$$

Integrated version of this equation 2.18 gives,

$$\ln k = \ln A - (E_a/RT) \tag{2.19}$$

where;

k = reaction rate constant (hr^{-1}),

A = frequency factor (hr^{-1}),

E_a = activation energy ($Jmol^{-1}$),

R = universal gas constant (8.314 $Jmol^{-1}K^{-1}$),

T = temperature (K).

The activation energy, E_a is obtained from a plot of ln$k$ against 1/T which will give an intercept of ln$A$ and a slope of (-E_a/R).

CHPATER THREE

3.0 MATERIALS AND METHODS

3.1 Apparatus

The glasswares used for this study were either S. Pyrex or Techmel products. The apparatus included a 3-neck flat bottom flask, magnetic stirrer hot plate 79-1, Brookfield viscometer, centrifuge machine, 2 magnetic bars, 500ml beakers, 250ml beakers, 500ml volumetric flasks,250ml Erlenmeyer flasks, 25ml pipettes, 50ml burette, 100ml, 250ml and 500ml measuring cylinders, 500ml separating funnels, glass thermometer (0 to 100 ^{o}C) and retort stands were used.

3.2 Methodology

3.2.1 Preparation of plantain peels ash

The ripe plantain peels samples were first collected from eateries and restaurants in Gidan Kwanu, Niger State and were washed with distilled water and then dried in an oven at 60 ^{o}C until they were dried enough for combustion. The samples were then burnt in an open air, with absolute caution, to prevent air current from blown off the ash. The resultant ash was carefully collected to minimize loss and stored in a polythene bag for the prospective extraction processes to be carried out (Efeovbokhan *et al.*, 2016).

3.2.2 Extraction of potassium hydroxide (KOH) from ripe plantain peels ash

The plantain ash sample was weighed (20 g each) and were added into the necessary volumes distilled water (10 ml/g ash) in 500 ml beakers. The mixture together with the container were then placed on a magnetic stirrer, with monitored stirring and heating at the temperature of 50 ^{o}C for a duration of 3 hrs. Filtration of the subsequent solution utilising a filter paper was carried out and after then, the produced solution was stored. The residue was then further extracted employing the above procedure. This procedure

was repeated until the solution from the residue tested approximately neutral to pH paper. Separate stainless-steel containers were used to collect the filtrates from every of the stages, respectively and each one of was evaporated to dryness in an oven. A plastic container was used to collect the weighed dried samples (Efeovbokhan *et al.*, 2016).

3.2.3 Rice husk preparation and pre-treatment

30 g of clean rice husk was stirred with 750 mL of 1.0 M H_2SO_4 at room temperature for 24h. The clean RH was treated with copious amount of mineral-free water to a constant pH. It was then dried in an oven at 100 °C for 24h (Thabet *et al*, 2015). The procedure was repeated for 6 separate times to obtain a reasonable amount of acid treated rice husk.

3.2.4 Preparation of KOH doped rice husk catalyst

3.2.4.1 catalyst A

The oven dried sample was burned in a muffle furnace at 600 ^oC for 4 hr so as to obtain white rice husk ash (Thabet *et al*., 2015). 30 g of KOH was impregnated by introducing it into 30 g of white rice husk ash and was allowed to age at room temperature for 18 hr. The resultant sample was dried in an oven at 110 ^oC for 24 hr and was finally calcined in a muffle furnace at 500 ^oC for 3 hr (Maniam, *et al*., 2015).

3.2.4.2 catalyst B

The 30 g of KOH was impregnated by introducing it into 30 g of the acid treated rice husk and the mixture was allowed to age at room temperature overnight. The gel was dried in an oven at 110 ^oC for 24 hr and was calcined in a muffle furnace at 600 ^oC for 4 hr (Thabet *et al*., 2015).

3.2.5 Characterisation of catalysts

The catalysts were characterized using Fourier Transform Infrared Spectroscopy (FTIR), X-ray Diffraction (XRD), Brunauer-Emmet-Teller (BET), Scanning Electron Microscopy (SEM) and Energy Dispersive X-ray (EDX).

3.2.6 Characterisation of castor oil

The castor oil was investigated for its specific gravity, flash point, kinematic viscosity, acid value, peroxide value, iodine value, moisture or water content and free fatty acid (FFA). The experimental description reported by the American Standards and Testing Materials (ASTM) were utilised in the determination of the above-mentioned properties.

3.2.6.1 specific gravity/density

A density bottle of volume, 25ml, was employed in the determination of the specific gravity of the oil sample. The weight of the empty density bottle, M_0 was recorded. The density bottle was filled with refined water and the freshly weighed, and the mass M_2 was noted. The bottle was emptied and dried in an oven. The dried bottle was then filled with castor oil and reweighed and the mass M_1 was also noted (Arawande and Akinnusotu, 2018). This procedure is according to ASTM D1298 standard. The result was calculated as below:

$$\text{Specific gravity} = \frac{M_1 - M_0}{M_2 - M_0} \quad (3.1)$$

3.2.6.2 determination of peroxide value

Rancidity which refers to the undesirable changes fats undergo as a result of storage which results to the development of unpleasant odour and taste and peroxide value of the oil is used to monitor this rancidity development through the peroxide evaluation. 20ml of a mixture of acetic acid and chloroform was prepared in a beaker and 1g of oil was measured out and mixed with 1g of potassium iodide and was introduced into the mixture.

The overall mixture was titrated with standard sodium thiosulphate solution using starch indicator (Arawande and Akinnusotu, 2018).

$$PV = \frac{(T_1 - T_2)\ x\ M\ x\ 1000}{W} \quad (3.2)$$

T_1 = Titre Value of sodium thiosulphate for blank test,

T_2 = Titre Value of sodium thiosulphate for the oil sample,

M = Normality of the standard sodium thiosulphate,

W = Weight of the oil used.

3.2.6.3 flash point determination

Cleveland open-cup method was employed to determine the flash point of castor oil. A reasonable amount of the oil sample was introduced into a test cup apparatus to desirable extent to reach the mark in the interior of the cup. The temperature of the cup content was slowly increased and the temperature, monitored with a thermometer until it has risen to a temperature of above 80^{o}C. At this point, the test flame (ignition source) was introduced at every temperature rise of 3^{o}C until it reached the temperature at which the first vapour ignition is noticed.

3.2.6.4 determination of viscosity

Brookfield Viscometer was utilised in the determination of the viscosity of the sample.

3.2.6.5 iodine value

The determination of the iodine value was carried out by treating 5g of the oil sample with surplus iodobromine (IBr) in freezing acetic acid. The mixture was titrated against standard sodium thiosulphate. The procedure was repeated for blank test (Arawande and Akinnusotu, 2018).

$$\text{IV} = \frac{126.9 \text{ x N x } (V_1 - V_2)\ x\ 100}{\text{M}} \quad (3.3)$$

N = Normality of sodium thiosulphate used,

V_1 = Volume of sodium thiosulphate used for the blank test,

V_2 = Volume of sodium thiosulphate used for sample,

M = Weight of oil sample.

3.2.6.6 moisture content

40g of the castor oil was weighed and dehydrated in an oven at a constant temperature of 105 °C for about 6 hrs. The sample was removed from the oven, left for 30 minutes to cool in a desiccator and weighed at 2hrs interval. This process was followed repeatedly until the sample recorded a constant weight (Arawande and Akinnusotu, 2018). The percentage water content of the oil was calculated from the formula:

$$\text{Moisture} = \frac{W_1 - W_2}{W_2}\ x\ 100\% \quad (3.4)$$

W_1 = Original weight of the sample before drying;

W_2 = Final weight of the sample.

3.2.6.7 acid value

The acid value is always represented as the percentage of FFA ASTM D664). 25 ml of diethyl ether was blended with 25ml of alcohol and some drops of phenolphthalein. The solution was cautiously mixed with 10g of castor oil and the resultant solution was titrated against aqueous 0.1M NaOH with constant shaking until a pink colour which perseveres for at least 15 seconds was noticed (Akpan, *et al.,* 2006). The 0.1M NaOH titre value (V_0) was taken. The Acid Value was calculated as:

$$\text{Acid value} = \frac{V_o \text{ x N x } 56.10}{W_o} \quad (3.5)$$

V_o = 0.1M NaOH titre value,

N = Normality of standard alkali used,

W_o = Weight of castor oil used.

$$FFA = \frac{\text{Acid Value}}{2} \quad (3.6)$$

3.2.7 Esterification of castor oil

Castor oil is very viscous in nature, and as such, will require pre-treatment as to make it suitable for biodiesel production via transesterification. The existence of high content of FFA in the crude castor oil is the reason double-step catalysed transesterification is used for the production of biodiesel. The initial step required is the esterification step needed to reduce the FFA so as to meet the required condition for biodiesel production. Esterification is the core treatment of the FFA in the oil which is high proceeded by the base catalysed transesterification of the oil that will convert the oil to biodiesel. This study esterified castor oil with H_2SO_4 so as to break the fatty acid present in the oil (Yacob *et al*., 2017).

3.2.8 Transesterification of castor oil

The transesterification of castor seed oil was first conducted to optimize the process parameters using the detailed design output of Response Surface Methodology of the design expert. Response Surface Methodology (RSM) embracing Randomised Optimal Design using three level-three factor design was used to optimize process conditions for the biodiesel production of castor oil using two different catalysts. Two responses termed yield A and yield B were obtained for the two different catalysts respectively. The software generated 20 experimental runs. The transesterification procedure was copied from Nurdin *et al*., (2015) and Yacob *et al*., (2017). The same procedure was used in the experimentation of the reusability of the catalyst employing the optimum conditions.

3.2.9 Kinetic study of transesterification of castor seed oil with methanol

For the kinetic study, 56.76 g of the castor seed oil and 284.94 g methanol were measured out into two distinct cleaned and dried beakers. 3.0wt/wt% of the catalyst B was made to solubilise in the ethanol and the consequential solution was then charged into a 3-necked flat bottom flask reactor and pre-heated to a temperature of 50 ^{o}C. The castor seed oil was also pre-heated to the same temperature in a separate beaker before being cautiously introduced into the solution in the reactor and then, was reacted at a temperature of 60 ^{o}C and 15ml solution was pipetted out of the reactor into a centrifugal tube at varying time of trans-esterification reactions from 0.5 hrs to 2.0 hrs at 30mins intervals. The procedure was repeated but with reaction temperatures of 61 ^{o}C and 62 ^{o}C respectively (Efeovbokhan *et al.*, 2017).

3.2.10 Catalyst reusability

For the purpose of industrialisation and commercialisation, reusability, recyclability and regeneration (3R) properties of a catalyst are of utmost importance. A study of the reusability of the catalyst has been carried out using the optimum transesterification conditions of 60^{o}C temperature, 6:1 methanol-oil molar ratio, 3 wt/wt% catalyst loading, 2 hours reaction time) (Hossain *et al.*, 2018). Recovery process was carried out after each run by washing the recovered catalyst with the help of a solvent (methanol) and drying the washed catalyst in an oven (Lani *et al.*, 2017).

CHPATER FOUR

4.0 RESULTS AND DISCUSSION

4.1 Catalyst Characterisation

The surface area, functional group, surface morphology and crystallinity of the synthesised catalysts as revealed by their characterisation are shown in the table below.

4.1.1 Brunauer-Emmet-Teller (BET) analysis

The catalysts were analysed with Brunauer-Emmet-Teller instrument known as SHIMADZU SS-100 using percentage of air permeability of the sample at constant pressure method. The data generated from the analysis are displayed in table 4.1 below.

Table 4.1: BET Analysis for Catalyst A and Catalyst B

Sample	**Specific Surface Area at 100 ^{o}C (m^2/g)**	**Pore Size Distribution at 40-100um (micron)**
Raw Rice Husk	60.10	48.20
Acid-Treated RH	60.70	45.00
KOH	77.52	50.20
Catalyst A	61.33	54.00
Catalyst B	71.33	54.20

The BET analysis of both catalysts A and B produced no appreciable difference in their pore size distribution, but Catalyst B had a higher specific surface area at 100 ^{o}C of 71.33 m^2/g than Catalyst B with 61.33 m^2/g. It also showed that the specific surface area and the pore size distributions of the synthesised catalysts were within the range of values reported by Nhung *et al.,* 2018 and Thabet *et al.*, 2015.

4.1.2 Fourier-transform infrared spectroscopy (FTIR) analysis

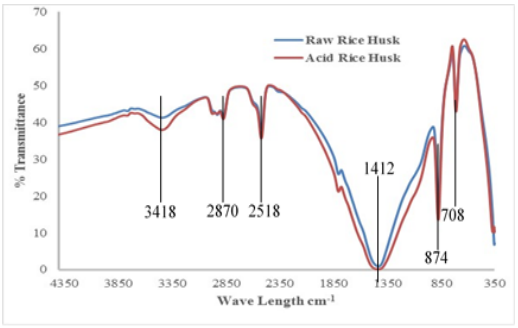

(4.1a)

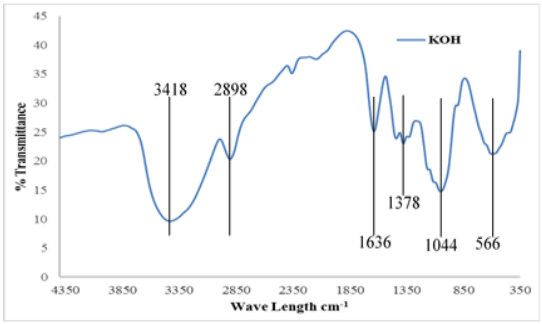

(4.1b)

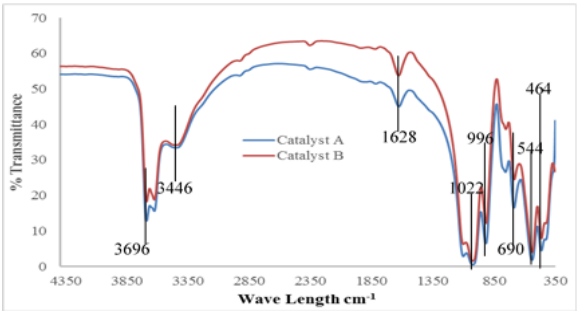

(4.1c)

Figure 4.1: FTIR Spectra of Raw Rice Husk and Acid-Leached Rice Husk (4.1a), KOH (4.1b), and Catalysts A and B (4.1c)

Figure 4.1a showed the IR spectra of both the raw rice husk and the acid-treated rice husk samples. Figure 4.1b showed the IR spectrum of the synthesised KOH. While Figure 4.1c showed the spectra of catalysts A and B. The peaks found within the region of 3700cm^{-1} – 3200cm^{-1} were due to the stretching vibrations of the O–H bonds of water molecules adsorbed onto the matrices of the samples (Muniandy *et al.,* 2014).

The weak bands found within 2800cm^{-1} – 3000cm^{-1} indicated the stretching vibrations of the C–H bonds of the methylene groups (CH_2) (Muniandy *et al.,* 2014).

The band at 1620cm^{-1} – 1680cm^{-1} were attributed to the stretching vibrations of C=C bands (alkene).

The band at 1378cm^{-1} – 1480cm^{-1} could be attributed to the bending vibrations of C–H band (alkane group). The vibrations noticed at 1022cm^{-1} - 1044cm^{-1} was as a result of the stretching vibrations of C-O bands of the ether group (Muniandy *et al.,* 2014).

4.1.3 Scanning electron microscopy (SEM) analysis

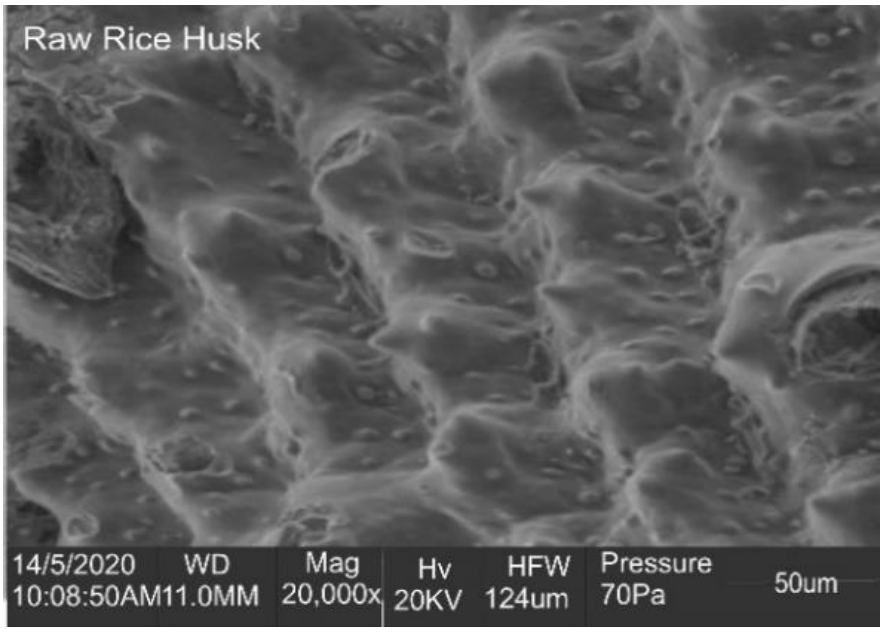

Figure 4.2: SEM micrograph of raw rice husk

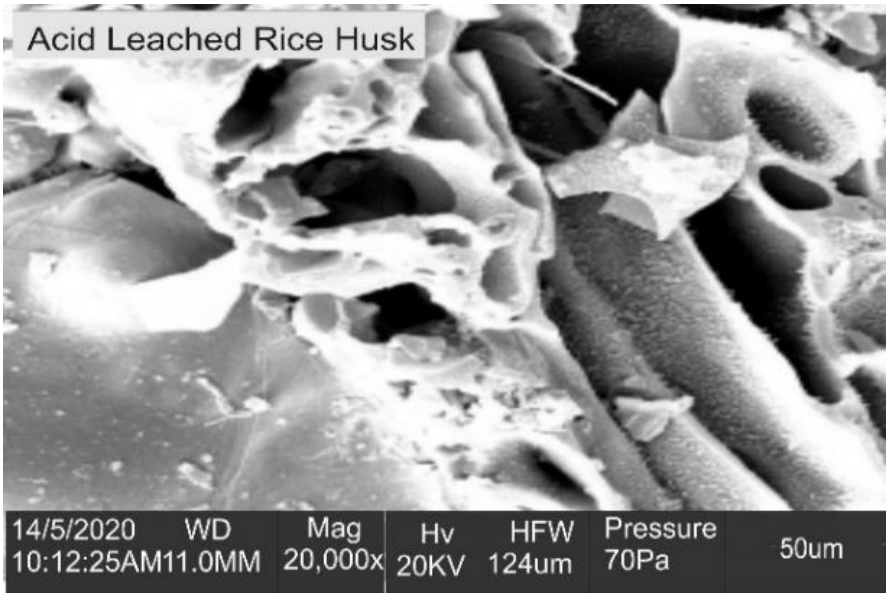

Figure 4.3: SEM micrograph of acid-leached rice husk

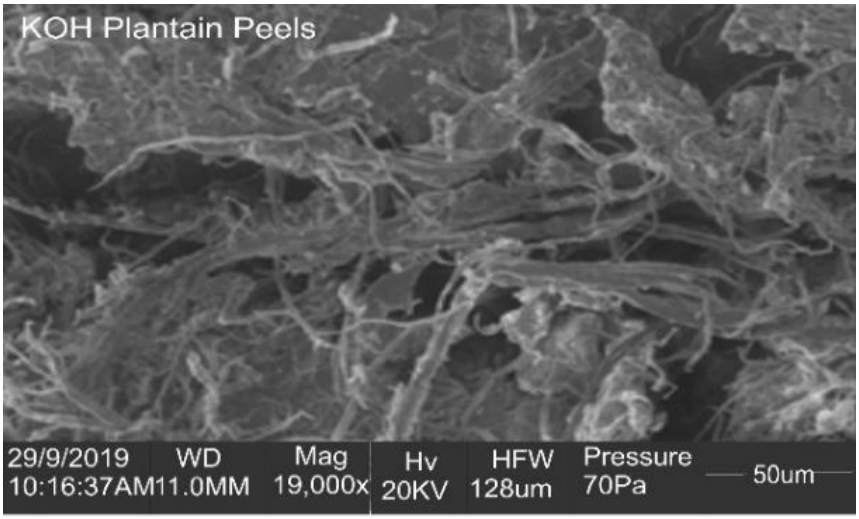

Figure 4.4: SEM micrograph of acid-leached rice husk

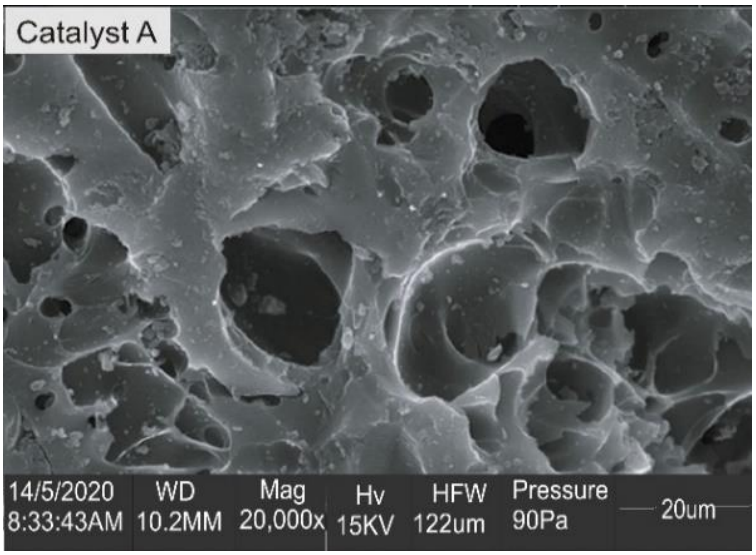

Figure 4.5: SEM micrograph of Catalyst A

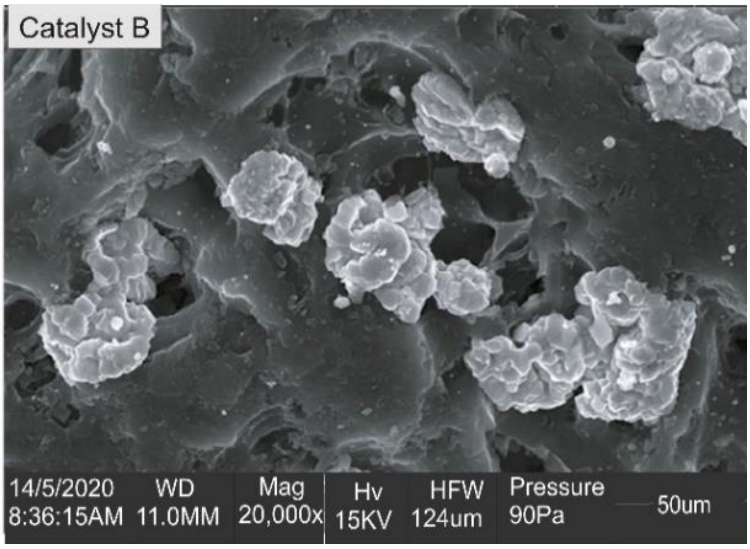

Figure 4.6: SEM micrograph of Catalyst B

Figure 4.2 exhibits the highly developed porous structure of the acid-leached rice husk sample from the relatively non-porous raw rice husk with corrugated structure (Figure 4.3). The acid leaching was confirmed to have induced the porosity of the rice husk material with high surface area and large pore volume. It was observed that the raw rice husk was fibrous and had no hollow structures could be attributed to the fact that the pores of the raw rice husk were filled with carbonaceous products (Touhami *et al.,* 2017). The calcination process showed more impact in figure 4.5 than in figure 4.6 which indicated that the pre-heat treatment process before doping is very important to increase the specific surface area of the samples. This conversion is ascribed to the decomposition of the volatiles due to the calcination process at high temperatures (Muniandy *et al.,* 2014).

The SEM micrographs of catalysts A and B were analysed using Image J software. Figure 4.7 show the SEM micrograph of catalyst A (4.7a), the sectioned portion of the micrograph that has gone through bandwidth filtering as well as thresholding (4.7b), and the sectioned portion showing the particle sizes (4.7c) while figure 4.8 show the SEM micrograph of catalyst B (4.8a), the sectioned portion of the micrograph that has gone through bandwidth filtering as well as thresholding (4.8b), and the sectioned portion showing the particle sizes (4.8c).

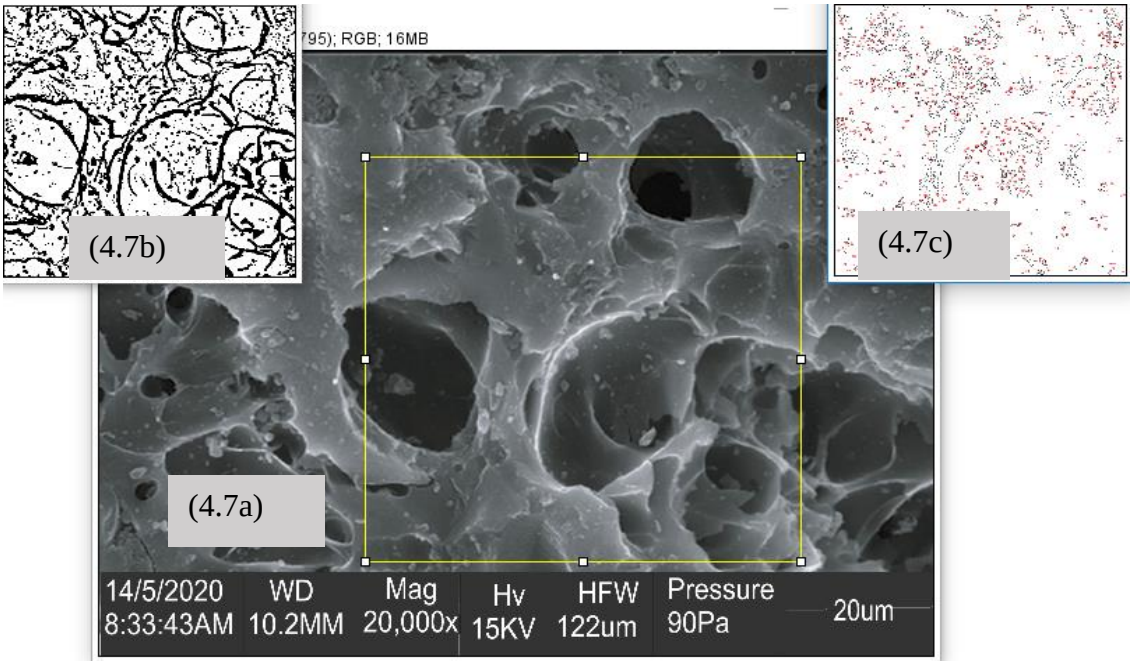

Figure 4.7: SEM micrograph of catalyst A analysed with ImageJ

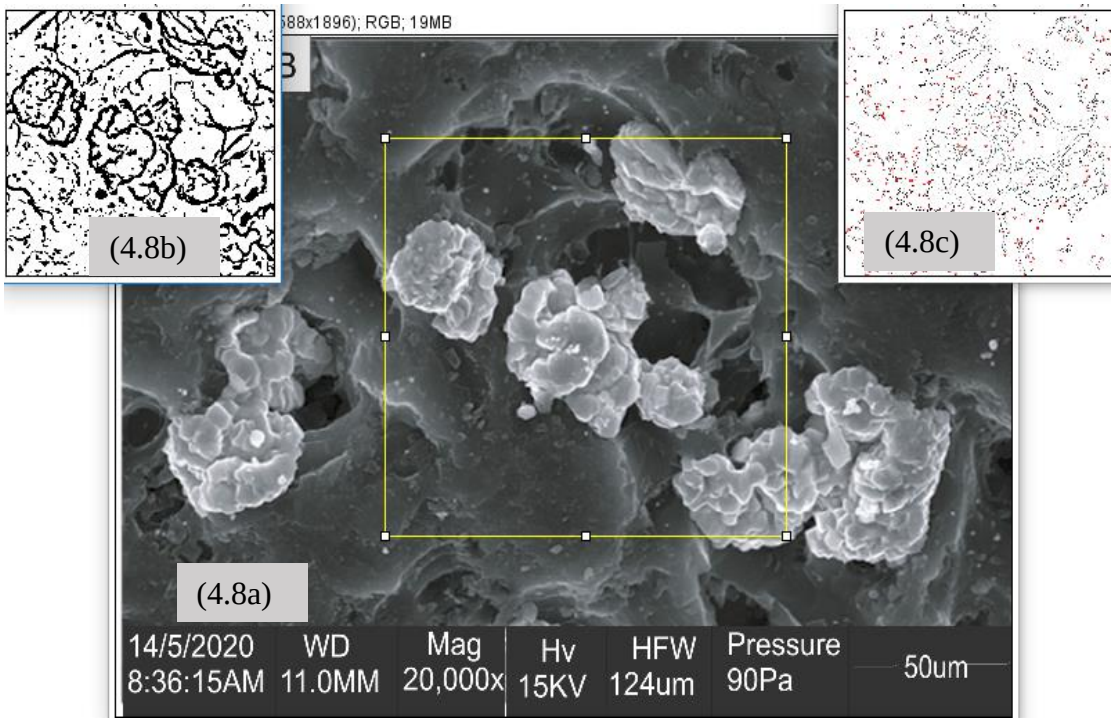

Figure 4.8: SEM micrograph of catalyst B analysed with ImageJ

Table 4.2: Summary of particle analysis using ImageJ software

Sample	Total Area	Average Size	%Area	Mean	Feret	Diameter
Catalyst A	373.241	0.444	11.097	255	0.89	21.7997
Catalyst B	2347.66	4.743	15.193	255	2.667	54.6730

The particle size distribution analysis was carried out on the two samples and the summary of the analysis is displayed in table 4.2. It can be deduced from the table 4.2 above that catalysed A had an average particle size of 0.444 µm which is far less than that of catalyst B with a particle size of 4.743 µm. The per centage area yielded by catalyst A is 11.10 while that of catalyst B is 15.19.

4.1.4 Energy dispersive X-ray (EDX) analysis

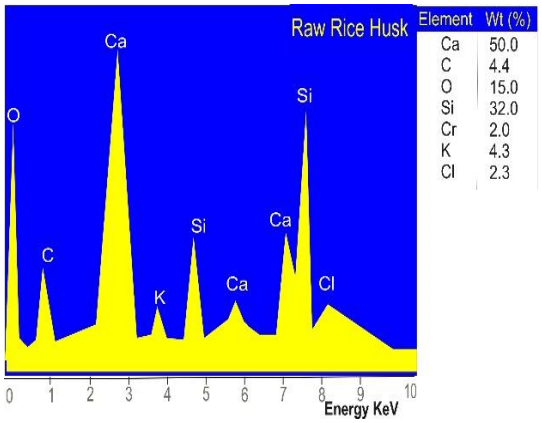

(4.9a)

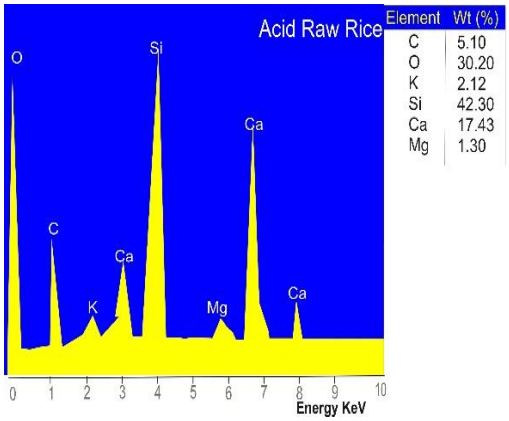

(4.9b)

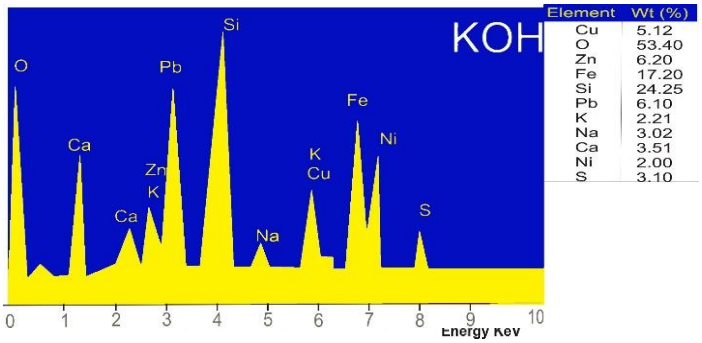

(4.9c)

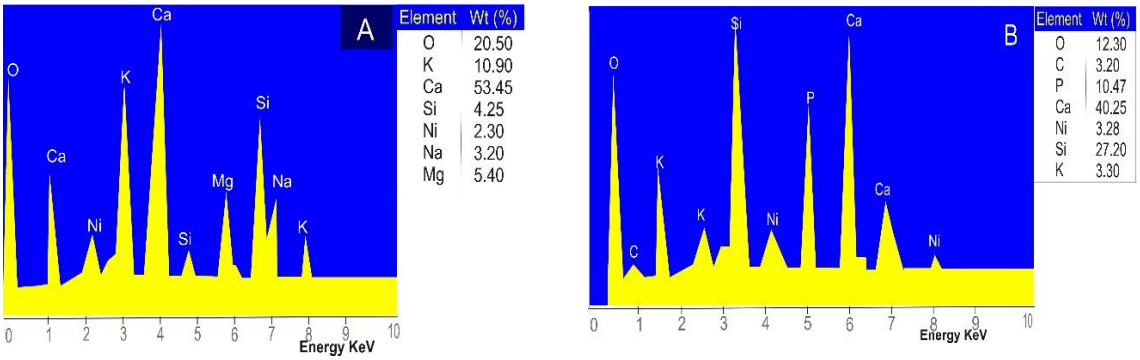

(4.9d) **(4.9e)**

Figure 4.9: Elemental Weight Composition of the Raw Rice Husk (4.9a), Acid-Leached Rice Husk (4.9b), KOH (4.9c), Catalyst A (4.9d) and Catalyst B (4.9e)

Table 4.3: Elemental weight composition of raw rice husk, acid-leached rice husk, KOH, catalysts A and B

Elements	Raw RH	Acid-Leached RH	KOH	Catalyst A	Catalyst B
			Weight (%)		
Si	32	42.3	24.25	4.25	27.2
Ca	50	17.43	3.51	53.45	40.25
Ni			2	2.3	3.28
Mg		1.3		5.4	
Na			3.02	3.2	
K	4.3	2.12	2.21	10.9	3.3
O	15	30.2	53.4	20.5	12.3
P					10.47
C	4.4	5.1			3.2
Cu			5.12		
Zn			6.2		
Fe			17.2		
Pb			6.1		
S			3.1		
Cr	2				
Cl	2.3				

The Energy Dispersive X-ray (EDX) of all the samples revealed the presence of several elements. The presence of silica was noticed in all the samples. It was observed in the acid-leached sample (4.9b) that the weight of Si increased from 32.0 wt(%) in raw rice

husk to 42.30 wt(%) after leaching while Catalyst B (4.9e) 27.20 wt(%) showed evidence of more Si content than Catalyst A (4.9d) 4.25 wt(%). KOH sample (4,9c) also displayed the presence of Si 24.25 wt(%). There is presence of Ni noticed in Catalysts A (2.3 wt%) and B (3.2 wt%) which could come from the KOH with wt(%) of 2. Also, the metal ions in the feedstocks (leached RH and KOH) like Mg and Na were no longer noticed in the catalyst B while they were noticed in catalyst A. However, the Energy Dispersive X-ray (EDX) also revealed the presence of other elements like Ca, O, and K in all the samples.

4.1.5 X-ray diffraction (XRD) analysis

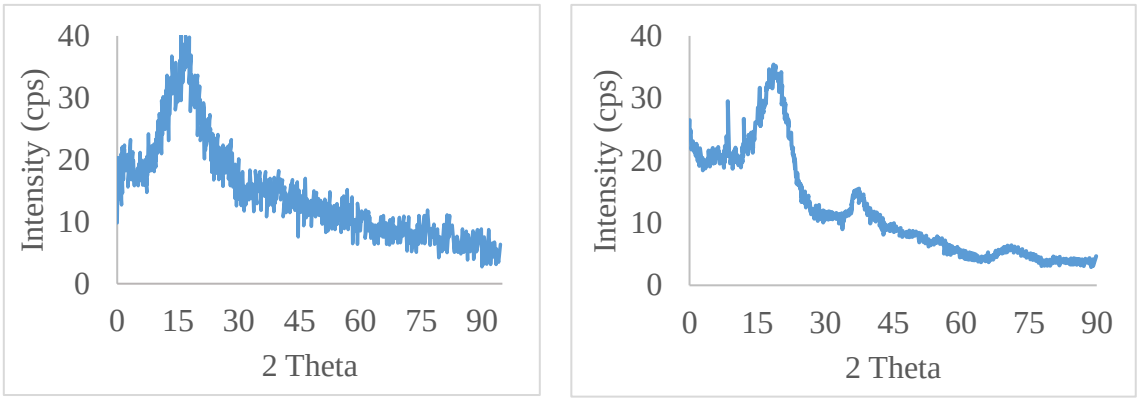

Catalyst A **Catalyst B**

Figure 4.10: X-ray Diffraction (XRD) diffractogram analysis of Catalysts A and B

The characteristic peaks at 2θ value obtained from the XRD diffractograms of both catalysts (A and B) at (7.3-31)° for catalyst A, and at (11.3-30)° and (35-43)° for catalyst B are similar as the typical KOH doped with rice husk peaks reported by Muniandy *et al.* (2014). The hunchbacks observed at these 2θ values are the characteristics of the amorphosity of the catalysts. The XRD patterns of the synthesised catalysts (A and B) are also similar to that reported by Touhami *et al.,* (2017). Muniandy *et al.,* (2014) reported that it could be right that there are some mark of micro-crystallinity with turbostratic graphite structure in the diffractogram of sample B at 2θ values of 8.5°. The broad nature

of the peak as reported by Touhami *et al.,* (2017) as seen at 2θ value at (7.3-31)° for catalyst A, and at (11.3-30)° and (35-43)° for catalyst B could be attributed to hydrogen bond transformation in cellulose during the heat treatment. Furthermore, the low crystallinity is believed to be due to the large amount of amorphous cellulose in the catalysts.

Analysing the X-ray Diffraction diffractograms of catalysts A and B using Origin App, utilising single peak – Gauss system under quick fit on the prominent peak on each catalyst XRDs, the parameters to calculate the crystallite sizes using Scherrer equation (equation 4.1) were generated.

$$\text{FWHM} = \frac{K\lambda}{LCos\theta} \quad (4.1)$$

Where:

FWHM = full width at half maximum (radian)

K = constant (0.94)

λ = constant (1.54178 Å)

L = Crystallite size (nm)

θ = angle (radian)

$$\text{Therefore, crystallite size, L} = \frac{K\lambda}{(FWHM)\ x\ Cos\theta} \quad (4.2)$$

Table 4.4: Generated data for the determination of crystallite size using Origin App

	K	**λ** (Å)	**Peak Position 2 Theta** (°)	**FWHM** (°)	**Crystallite Size** (nm)
Catalyst A	0.94	1.54178	16.30794	9.75222	0.86017
Catalyst B	0.94	1.54178	17.99761	9.88212	0.85075

Hence, catalyst A has a crystallite size of 0.86017 nm while catalyst B has a crystallite size of 0.85075 nm.

4.2 Optimization of the Process Conditions using Response Surface Methodology

4.2.1 Analysis of variance (ANOVA) and model fitting

Response Surface Methodology (RSM) embracing Randomised Optimal Design using three level-three factor design was used to optimize process conditions for the biodiesel production of castor oil using two different catalysts. The experimental constraints, choices and levels of independent variables studied and the corresponding results of the optimal design are shown in Table 4.5. Design-Expert® software Version 11 was used to analyse the results of the twenty experiments obtained employing Response Surface Methodology with optimal design. Two responses termed yield A and yield B were obtained for the two different catalysts respectively. From the design experiment, quadratic polynomial equations comprising three linear coefficients (A, B, C), three interfacial coefficients (AB, AC, BC) and three quadratic coefficients (A2, B2, C2) were attained for the FAME yield predictions in terms of coded and actual factors as represented by Tables 4.3 and 4.4.

Table 4.5: Final equations in terms of coded and actual factors for biodiesel yield using catalyst A

Coded Factors	**Actual Factors**
1/Sqrt(Yield A) =	1/Sqrt(Yield A) =
+0.1211	+1.46848
-0.0058 A	+0.009585 Catalyst Loading
-0.0017 B	-0.044584 Temperature
-0.0008 C	+0.000088 Time
+0.0000 AB	+7.33358E-06 Catalyst Loading * Temperature
+0.0006 AC	+0.000043 Catalyst Loading * Time
-0.0003 BC	-1.88549E-06 Temperature * Time
-0.0013 A^2	-0.005080 Catalyst Loading^2
+0.0092 B^2	+0.000370 Temperature^2
-0.0005 C^2	-6.06132E-07 Time^2

Table 4.6: Final equations in terms of coded and actual factors for biodiesel yield using catalyst B

Coded Factors	Actual Factors
1/Sqrt(Yield B) =	1/Sqrt(Yield B) =
+0.1131	+1.05970
-0.0060 A	-0.001921 Catalyst Loading
-0.0011 B	-0.030417 Temperature
-0.0014 C	-0.000182 Time
-0.0001 AB	-0.000053 Catalyst Loading * Temperature
+0.0005 AC	+0.000035 Catalyst Loading * Time
-0.0000 BC	-2.11326E-07 Temperature * Time
-0.0005 A^2	-0.001982 Catalyst Loading^2
+0.0063 B^2	+0.000253 Temperature^2
+0.0003 C^2	+3.38215E-07 Time^2

Tables 4.5 and 4.6 display the equations in terms of coded and actual factors for biodiesel yield using catalysts A and B respectively. The equations for coded factors are put to use for predicting the yields for given levels of each factor. The high factor levels are, by default, coded as +1 whereas the low levels are coded as -1. The relative impacts of the factors can be identified by running an appreciable comparison on the factor coefficients. In the same vein, the equations for actual factors are put to use for predicting the biodiesel yield for given levels of each factor. In this case, the factors are specified in the original units as every factor bears. These equations are not suitable for the prediction of the relative impact of each factor because the intercept is not located at the centre of the design space and the coefficients are made in such a way to accommodate the units of each factor. Nevertheless, the only terms included in the above Tables (4.5) and (4.6) are terms with p-value < 0.05 which, in other words, are significant terms. The analysis of variance (ANOVA) employing REML (REstricted Maximum Likelihood) as well as fit statistics of the model were statistically analysed.

Table 4.7: The optimal experimental design of castor oil transesterification using two different catalysts and results

Run	*A:Catalyst Loading* (% wt/wt)	*B:Temperature* (ºC)	*C:Time* (minutes)	*Yield A* (%)	*Yield B* (%)
1	2.5	60	120	69.55	79.95
2	3	60	90	76.75	87.98
3	2	65	90	56.31	65.48
4	3	55	60	64.79	75.18
5	2	60	60	63.22	68.82
6	3	65	60	67.75	78.44
7	3	55	60	64.79	75.18
8	2	60	120	65.64	72.88
9	2.5	65	90	60.63	71.32
10	2	65	60	55.34	62.68
11	2.5	60	60	67.6	75.82
12	2	65	60	55.34	62.68
13	2.5	55	120	58.61	70.22
14	2	55	120	54.83	64.97
15	2	55	60	52.83	61.07
16	3	60	90	76.75	87.98
17	3	60	120	77.76	88.92
18	3	65	60	67.75	78.44
19	3	65	120	68.94	80.99
20	2	55	90	53.81	62.98

Table 4.7 shows the number of experimental runs with varying factors of catalyst loading (wt/wt %), reaction temperature (^{o}C) and reaction time (mins) as well as two experimental responses termed Yield A and Yield B representing the yield of biodiesel using catalysts A and B respectively. From the data obtained, it was established that reaction conditions of temperature (60 ^{o}C), catalyst loading (3 wt/wt%) and time (120 mins) gave the optimum yield for the both catalysts whereas the reaction conditions of temperature (55 ^{o}C), catalyst loading (2 wt/wt%) and time (60 mins) produced the minimum biodiesel yield for the two catalysts as well.

Table 4.8: Analysis of variance (ANOVA) for Yield A

Source	Sum of Squares	df	Mean Square	F-value	p-value	
Model	0.0011	9	0.0001	1049.38	< 0.0001	significant
A-Catalyst Loading	0.0004	1	0.0004	3300.36	< 0.0001	
B-Temperature	0.0000	1	0.0000	212.87	< 0.0001	
C-Time	7.963E-06	1	7.963E-06	67.01	< 0.0001	
AB	3.259E-09	1	3.259E-09	0.0274	0.8718	
AC	3.580E-06	1	3.580E-06	30.13	0.0003	
BC	5.348E-07	1	5.348E-07	4.50	0.0599	
A^2	4.692E-06	1	4.692E-06	39.49	< 0.0001	
B^2	0.0003	1	0.0003	2826.35	< 0.0001	
C^2	1.052E-06	1	1.052E-06	8.86	0.0139	
Residual	1.188E-06	10	1.188E-07			
Lack of Fit	1.188E-06	6	1.980E-07			
Pure Error	0.0000	4	0.0000			
Cor Total	0.0011	19				
C.V.% = 0.2742; R^2=0.9989; Adjusted R^2=0.9980; Predicted R^2=0.9954; Std. Dev.=0.0003; Mean=0.1257; Adeq Precision=97.9572						

Tables 4.8 and 4.9 show that the p-values of the models of the two responses are all significant in predicting the response and suitability of the models with values of p-values less than 0.0001. The F-values of the models are 1049.38 and 2949.33 for Yield A and Yield B respectively. The results above approve the significance of the fitted models for there exist only a 0.01% chance that F-values as high as these could be caused by noise. The coefficient of variation for the two responses are extremely small (CV = 0.2742% for Yield A and 0.1596 for Yield B) indicating the reliability of the fitted model. The degree of the fitness of the model was assessed with the coefficient of variation (R^2 = 0.9989 for Yield A and R^2 = 0.9996 for Yield B which suggest that 99.89% and 99.96% of the

respective experimental data are compatible with the data predicted by the model). The evaluation of the p-values of each coefficient of the model provided that A, B, C, AC, A^2, B^2 and C^2 are significant model terms while AB and BC are insignificant for both yield A and yield B.

Table 4.9: Analysis of variance (ANOVA) for Yield B

Source	Sum of Squares	df	Mean Square	F-value	p-value	
Model	0.0009	9	0.0001	2949.33	< 0.0001	significant
A-Catalyst Loading	0.0004	1	0.0004	11955.62	< 0.0001	
B-Temperature	0.0000	1	0.0000	295.29	< 0.0001	
C-Time	0.0000	1	0.0000	670.01	< 0.0001	
AB	1.730E-07	1	1.730E-07	4.95	0.0503	
AC	2.382E-06	1	2.382E-06	68.14	< 0.0001	
BC	6.719E-09	1	6.719E-09	0.1922	0.6704	
A^2	7.145E-07	1	7.145E-07	20.45	0.0011	
B^2	0.0002	1	0.0002	4491.80	< 0.0001	
C^2	3.277E-07	1	3.277E-07	9.38	0.0120	
Residual	3.495E-07	10	3.495E-08			
Lack of Fit	3.495E-07	6	5.825E-08			
Pure Error	0.0000	4	0.0000			
Cor Total	0.0009	19				

C.V.% = 0.1596; R^2=0.9996; Adjusted R^2=0.9993; Predicted R^2=0.9982;
Std. Dev.=0.0002; Mean=0.1172; Adeq Precision=166.3610

4.2.2 Effects of the process variables on the yield of biodiesel

The response surface plots were drawn with the help of the Design Expert software. The effect and/or the significant relations between constraints involved were evaluated using 3D surface and Contour plots. The effect of the process parameters on the yield of the

biodiesel, where two sovereign variables were varied while a variable was held constant for each contour plot were evident from the plots. In the final quadratic model equation to check the effect of autonomous parameters on the FAME yield, only the terms with p-value < 0.05, based on 95% confidence limit, were included. The reduced significant quadratic models are shown below:

$$Z_A = 0.1211 - 0.0058A - 0.0017B - 0.0008C + 0.0006AC - 0.0013A^2 + 0.0092B^2 - 0.0005C^2 \quad (4.3)$$

$$Z_B = 0.1131 - 0.0060A - 0.0011B - 0.0014C + 0.0005AC - 0.0005A^2 + 0.0063B^2 + 0.0003C^2 \quad (4.4)$$

Consequently, all the linear terms, interactive terms between catalyst loading and time and quadratic terms of catalyst loading, temperature and time (A, B, C, AC, A^2, B^2 and C^2) were statistically significant for both models. Nevertheless, all other relational terms (i.e. AB and BC) were not statistically significant for both models.

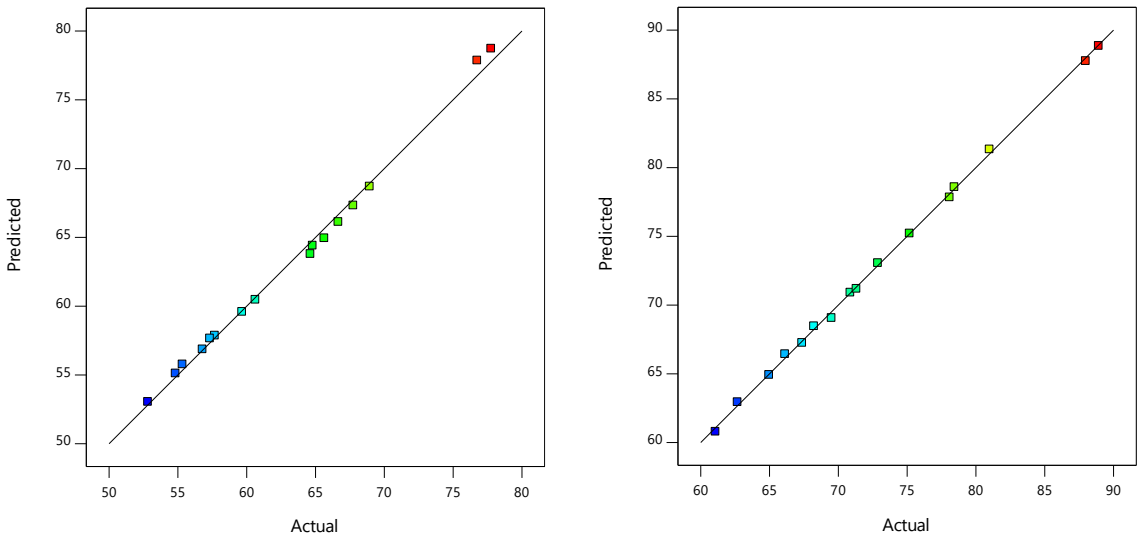

Figure 4.11: Comparison of predicted yields against actual yields for Catalysts A and B respectively.

Table 4.10: Predicted vs Experimental yields of biodiesel for catalysts A and B

Run	Experimental (Yield A)	Predicted Yield A	Experimental (Yield B)	Predicted Yield B
1	69.55	69.8015	79.95	79.7903
2	76.75	76.9157	87.98	87.9842
3	56.31	56.4454	65.48	65.1418
4	64.79	64.7131	75.18	75.1958
5	63.22	62.505	68.82	68.5643
6	67.75	67.717	78.44	78.3841
7	64.79	64.7131	75.18	75.1958
8	65.64	65.5043	72.88	73.1867
9	60.63	60.4493	71.32	71.4499
10	55.34	55.4395	62.68	62.8148
11	67.6	67.9126	75.82	75.8979
12	55.34	55.4395	62.68	62.8148
13	58.61	58.3427	70.22	70.1577
14	54.83	55.0307	64.97	64.8308
15	52.83	53.1503	61.07	61.0266
16	76.75	76.9157	87.98	87.9842
17	77.76	77.9154	88.92	88.9702
18	67.75	67.717	78.44	78.3841
19	68.94	68.7795	80.99	81.0265
20	53.81	53.647	62.98	63.1903

Table 4.10 displays the experimental biodiesel yield in comparison with the model predicted biodiesel yield using catalysts A and B and these data were extracted from Figure 4.11. The results show that there are only fractional differences in the FAME yields from the experiments and that predicted by the models for the both catalysts.

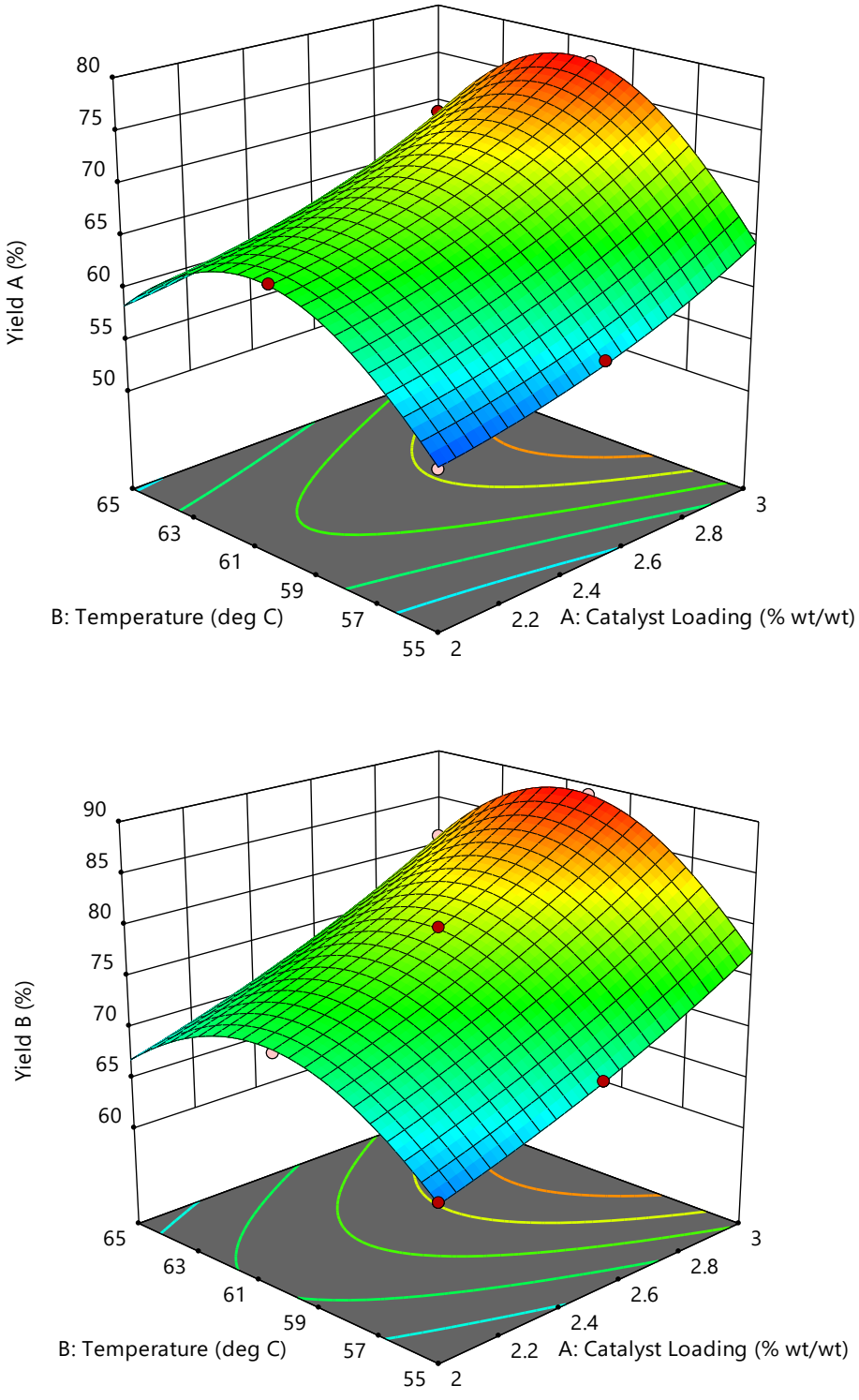

Figure 4.12: The 3D plots of Temperature and Catalyst Loading Fame yields for Catalysts A and B respectively.

Figure 4.12 shows the 3D plots for the FAME yields of produced biodiesel using the two different catalysts at varying conditions of temperature and catalysts loading and a constant time of 120 mins. On both catalytic accounts, the temperature effect on biodiesel yield were noticed with curvilinear temperature that had positive quadratic coefficients and negative linear coefficients. The catalyst loading increased with increase in yield on the two accounts with negative quadratic and linear coefficients. However, there was no clear interaction between the two factors as they showed independent relationship because there is no noticeable convergence even at their zero levels.

4.2.3 Optimization of the process parameters for the castor oil transesterification

The regression equation was solved with the help of the Design Expert and the optimal values were obtained for the three independent process factors. The software produced 100 different optimized values but the 25^{th} value was chosen to be the best out of all as it gave the maximum FAME yield. The goals of the three independent process variables, the % yield of the FAMEs, the lower and upper weights and the importance were set to "in range", "maximise", "1" and "3" respectively (Table 4.11).

Table 4.11: Optimization of Castor Oil Transesterification Process Factors under Optimum Conditions

Name	Goal	Lower Limit	Upper Limit	Lower Weight	Upper Weight	Importance
A:Catalyst Loading	is in range	2	3	1	1	3
B:Temperature	is in range	55	65	1	1	3
C:Time	is in range	60	120	1	1	3
Yield A	minimize	0.113402	0.137581	1	1	3
Yield B	minimize	0.106047	0.127963	1	1	3

Table 4.12: Solutions of the Optimization of Castor Oil Transesterification Process Factors under Optimum Conditions

Solution Number	Catalyst Loading	Temperature	Time	Yield A	Yield B	Desirability	Status
			Prediction				
1	2.999	60.35	119.96	78.02	89.05	1	Selected
			Experimental				
	2.999	60.35	119.96	78.01	89.02		

The predictions made, from the model, for the optimal values are as shown in Table 4.12. The model predicted optimum biodiesel yields under these optimum process conditions are, yield A (78.0249%); yield B (89.0509%).

The results predicted by the model were validated by carrying out laboratory investigations using the optimum parameters. The laboratory result showed FAME yields of 78.01 and 89.02 for yield A and yield B respectively. These results are in close conformity with the model predictions.

4.3 Kinetic Study of the Transesterification of Castor Seed Oil

4.3.1 Determination of the reaction conversions

Table 4.13: The volume of biodiesel produced at catalyst loading of 3.0 wt/wt%, methanol-to-oil molar ratio of 6:1 & temperatures of 60^{o}C, 61^{o}C and 62^{o}C

Time, t_f	Volume of biodiesel (g)		
(hrs)	Temperature of 60^{o}C	Temperature of 61^{o}C	Temperature of 62^{o}C
0.5	8.855	7.45	5.925
1.0	11.864	11.176	11.103
1.5	12.118	11.91	11.453
2.0	13.289	12.824	12.580

Table 4.14: The conversions obtained from the experimental data

Time, t_f	Conversion, X_{Af}		
(hrs)	**Temperature of 60 ºC**	**Temperature of 61 ºC**	**Temperature of 62 ºC**
0.5	0.6227	0.5239	0.4167
1.0	0.8543	0.7859	0.7808
1.5	0.8722	0.8376	0.8054
2.0	0.9345	0.9018	0.8847

4.3.2 Determination of reaction rate constants

Table 4.15: The evaluation of $(1-X_{Af})$ for the conversions

Time, t_f	$(1-X_{Af})$	$(1-X_{Af})$	$(1-X_{Af})$
(hrs)	**Temperature of 60 ºC**	**Temperature of 61 ºC**	**Temperature of 62 ºC**
0.5	0.3773	0.5833	0.5833
1.0	0.1457	0.2192	0.2192
1.5	0.1278	0.1946	0.1946
2.0	0.0655	0.1153	0.1153

Table 4.16: The evaluation of $\ln(1-X_{Af})$

Time, t_f	$\ln(1-X_{Af})$	$\ln(1-X_{Af})$	$\ln(1-X_{Af})$
(hrs)	**Temperature of 60 ºC**	**Temperature of 61 ºC**	**Temperature of 62 ºC**
0.5	-0.975	-0.742	-0.539
1.0	-1.926	-1.575	-1.518
1.5	-2.057	-1.818	-1.637
2.0	-2.726	-2.321	-2.160

A close examination of data in table 4.14 revealed that the FAME conversion is a function of time as the castor oil conversion increased from 0.6227 to 0.9345 as the time was increased from 0.5 hrs to 2.0 hrs at a constant oil-to-methanol ratio, temperature and catalyst loading of 6:1, 60 ºC and 3 wt/wt% respectively. The conversion of castor oil followed a similar trend, when the temperature of reaction was increased to 61 and 62 ºC, respectively, while other reaction conditions were maintained, as it increased from 0.5239 to 0.9018 and from 0.4167 to 0.8847 respectively.

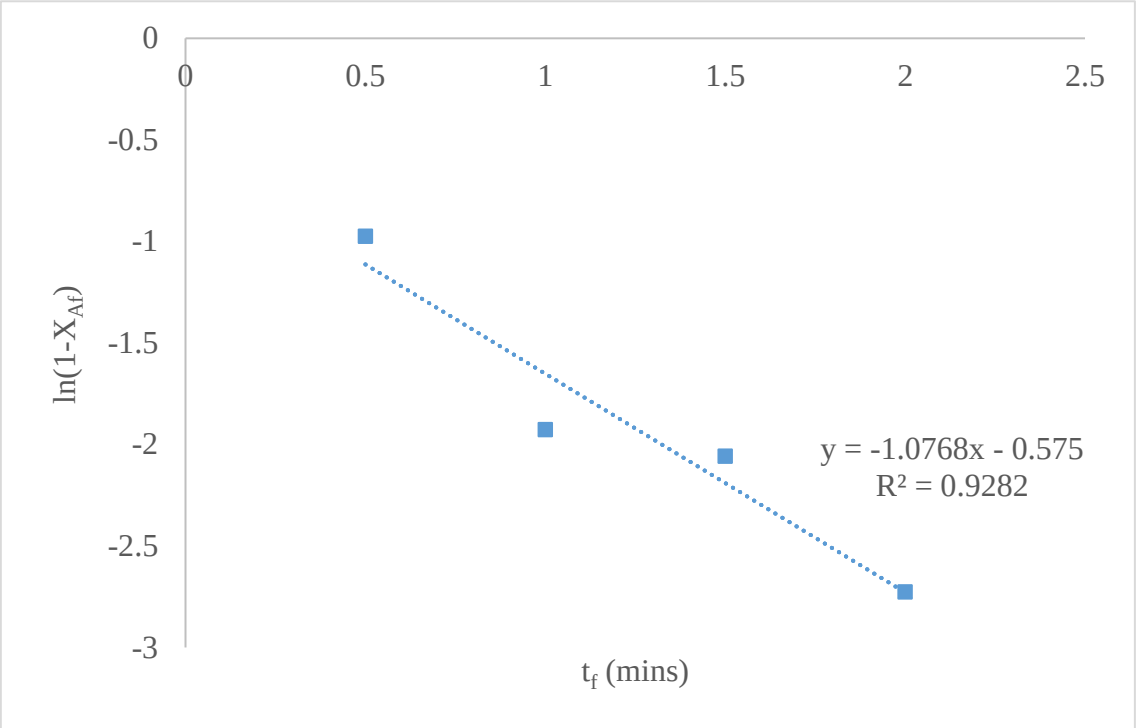

Figure 4.13: The plot of $\ln(1-X_{Af})$ against t_f (hrs) at temperature of 60 ^oC.

Calling up equation 2.17, the plot of t_f against $\ln(1-X_{Af})$ produced a straight line with a retarding slope at the three different temperatures as was reported by Efeovbokhan *et al* (2017) [Figures 4.13, 4.14 and 4.15]. The model equations for the three different plots are represented below:

For 60^{o}C: y = -1.0768x - 0.575 (4.5)

For 61^{o}C: y = -1.0028x - 0.352 (4.6)

For 62^{o}C: y = -0.9964x - 0.218 (4.7)

From equation 4.5, the slope of the plot is -1.0768 = $-\frac{1}{K_1}$.

Therefore, *k* at 60^{o}C = $(1.0768)^{-1}$ = 0.9287 hr^{-1}. This implies that from "equation 11", the pseudo first order reaction rate law of the transesterification of castor oil at 60 ^{o}C to fatty acid methyl ester using synthesised plantain peels potassium hydroxide (KOH) doped on rice husk $-r_A = 0.9287C_A$. (4.8)

Similarly, from equation 4.6, the slope of the plot is -1.0028 = $-\frac{1}{K_1}$.

k at 61 ^{o}C = $(1.0028)^{-1}$ = 0.997 hr^{-1}. This also implies that from "equation 11", the pseudo first order reaction rate law of the transesterification of castor oil at 61 ^{o}C to fatty acid methyl ester using synthesised plantain peels potassium hydroxide (KOH) doped on rice husk $-r_A = 0.997C_A$. (4.9)

Also, from equation 4.7, the slope of the plot is = -0.9964= $-\frac{1}{K_1}$.

k at 62 ^{o}C = $(0.9964)^{-1}$ = 1.004 hr^{-1}. This also implies that from "equation 11", the pseudo first order reaction rate law of the transesterification of castor oil at 62 ^{o}C to fatty acid methyl ester using synthesised plantain peels potassium hydroxide (KOH) doped on rice husk $-r_A = 1.004C_A$. (4.10)

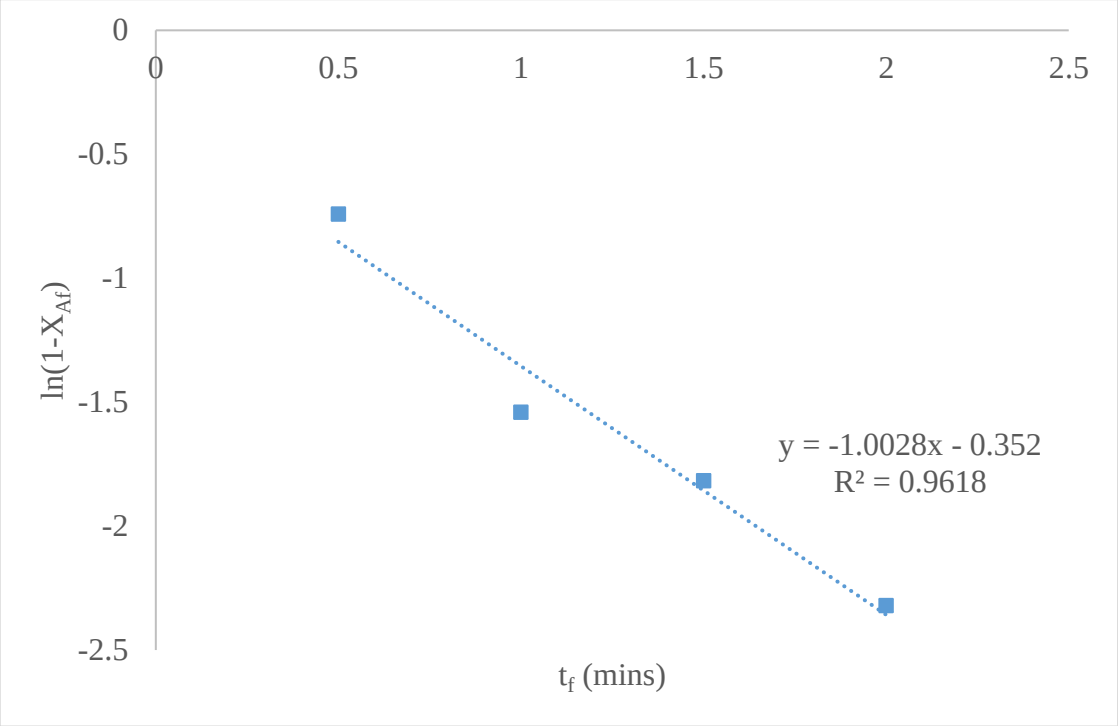

Figure 4.14: The plot of ln(1-X_{Af}) against t_f at temperature of 61 ^{o}C.

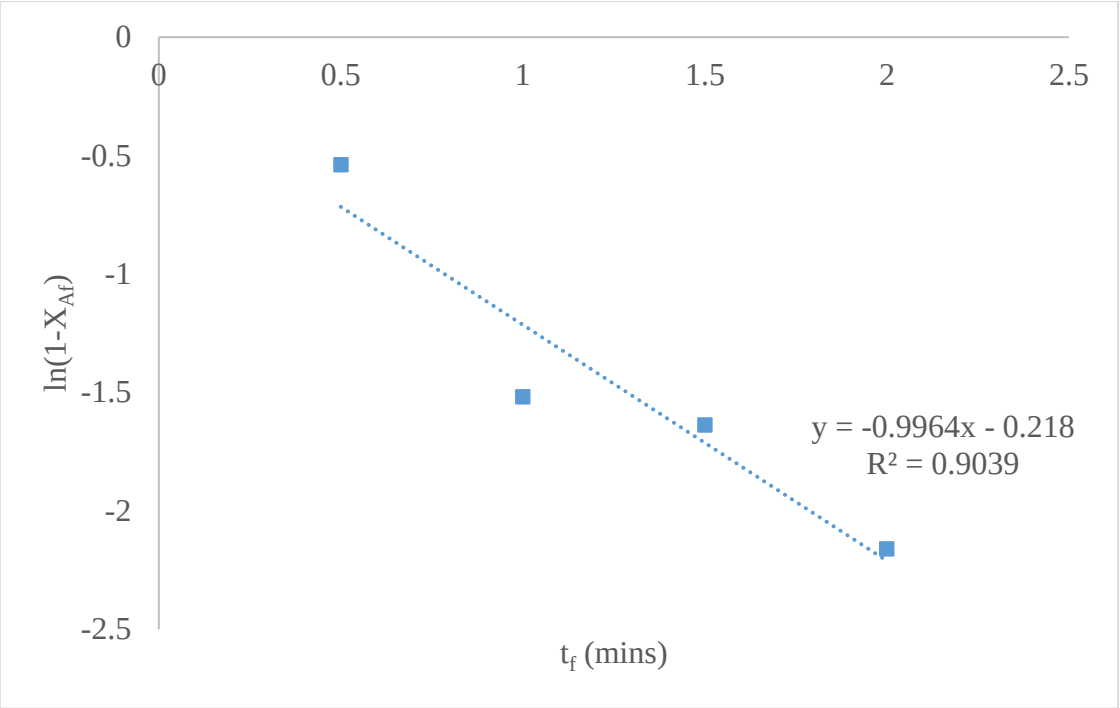

Figure 4.15: The plot of $\ln(1-X_{Af})$ against t_f at temperature of 62 ^oC.

By implication, equations (4.8), (4.9) and (4.10), as well as the experimental plots (Figures 4.13, 4.14 and 4.15) and the experimental data are in great conformity with the rate law and rate constant of the first order reaction. This goes a long way to show that the trans-esterification of castor oil to fatty acid methyl ester using synthesised plantain peels potassium hydroxide (KOH) doped on rice husk is a first order reaction regarding castor seed oil with methanol molar ratio extremely kept constant in large excess.

4.3.3 Determination of reaction activation energy

As earlier stated in chapter two, the activation energy of the transesterification reaction of castor seed oil using synthesised plantain peels potassium hydroxide (KOH) doped on rice husk as a catalyst and methanol as the alcohol is determined by a plot of ln*k* against 1/T from the Arrhenius relation according to Equation 2.19.

Table 4.17 shows the temperatures of reactions in K and the corresponding *k*-values in hr^{-1}. Table 4.18 shows the inverse of the absolute temperatures of reaction and the logarithm values of the k-values.

Table 4.17: The temperatures of reaction (K) and corresponding *k*-values (hr^{-1})

Temperature (K)	***k*-values (hr^{-1})**
333	0.9287
334	0.997
335	1.004

Table 4.18: The evaluation of ln*k* and 1/T

1/T	**ln*k***
0.003003	-0.074
0.002994	-0.003
0.002985	0.004

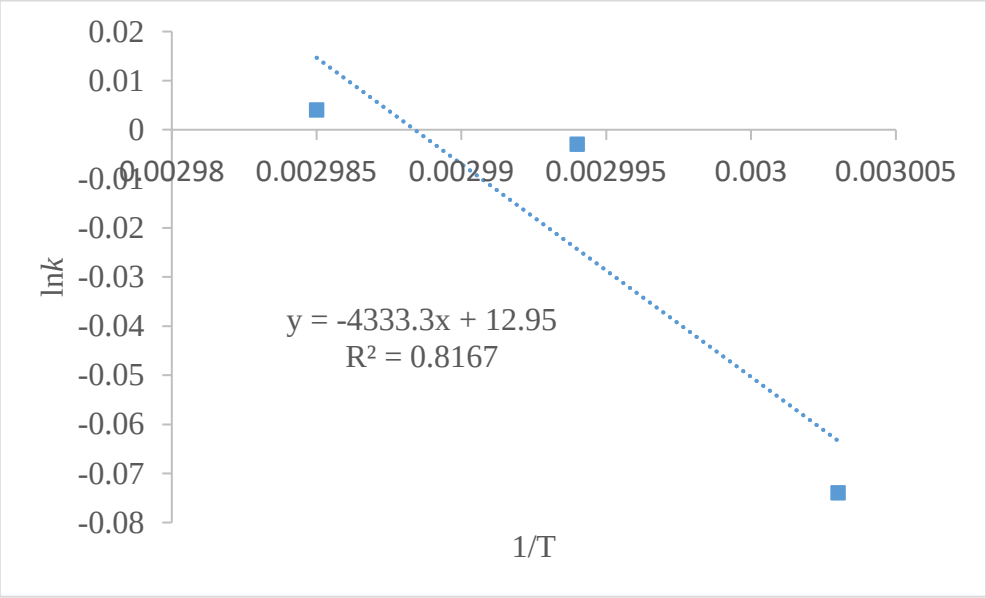

Figure 4.16: The plot of ln*k* against 1/T

From the model equation in the Figure 4.16 above, the slope of the plot,

($-E_a$/R) = -4333.3 K => E_a = (4333.3 x 8.314) $Jmol^{-1}$ = 36,027.06 $Jmol^{-1}$ (36.03 KJ/mol).

The intercept ln$A$ = 12.95 hr^{-1}.

The above activation energy is way higher than that reported by Sarve *et al.*, 2015. This might be as a result of high viscosity and higher fatty acid profile of castor seed oil.

4.4 Biodiesel Production

Comparison of the produced biodiesel with the standard exposed that it is in conformity with the standard as shown in Table 4.19.

Table 4.19: The conformity of Synthesised Biodiesel with the Standard Biodiesel

Properties	**Units**	**Castor Oil FAME**	**ASTM D6751**
Density 40°C	g/cm^3	0.956	-
Kinematic Viscosity at 40°C	mm^2/s	5.4	1.9 – 6.0
Flash Point	-	135	130 min
Pour point	° C	-5	-
Cetane Index	-	51	47 min
Cloud point	-	6 ° C	-
Iodine value	mg I/100g	86	-
Ester value	wt. %	99.4	-
pH Value	-	7.38	-
Biodiesel Yield	%	88.92	-

4.5 Catalyst Reusability

Heterogeneous catalysts and their importance in the commercialisation of biodiesel production in terms of their recyclability, reusability and regeneration (3R) is enormous.

A study of the reusability of the catalyst has been carried out using the optimum transesterification conditions of 60 ^{o}C temperature, 6:1 methanol-oil molar ratio, 3 wt/wt% catalyst loading, 2 hours reaction time).

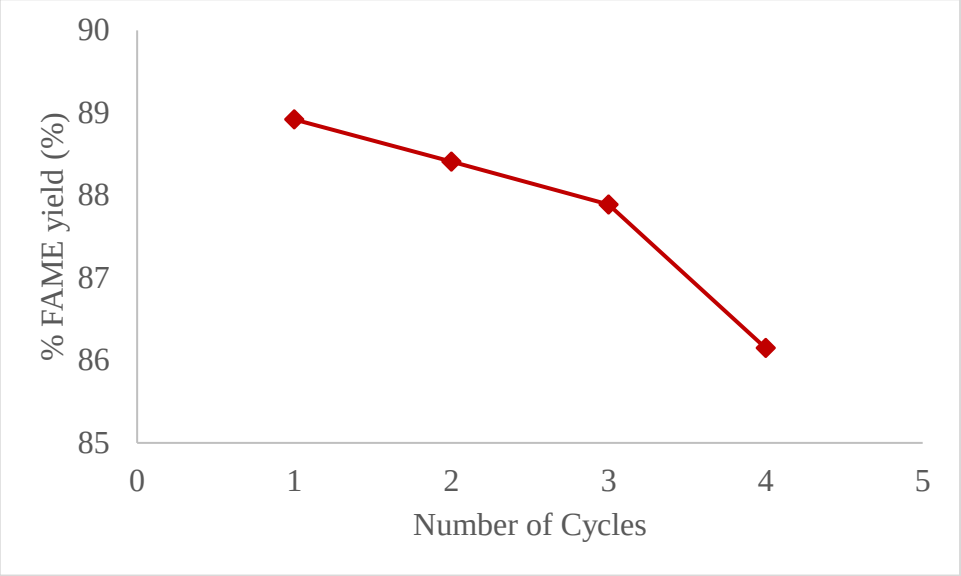

Figure 4.17: Catalyst reusability curve

The catalyst was subjected to reuse for 4 consecutive times and the result displayed that as the number of cycles progressed, the yield slightly reduced as shown in Figure 4.17. This slight reduction in yield could be attributed to any of the following: blockage of the active sites by glycerol or biodiesel or the presence of non-reacted oil or carbon deposits on the same active sites (Lani *et al.*, 2017) or due to the degradation of the active sites by leaching (Hossain *et al.*, 2018).

CHAPTER FIVE

5.0 CONCLUSION AND RECOMMENDATIONS

5.1 Conclusion

The Characterisation of both catalysts A and B has shown the activity of both catalysts. This fact was validated by the BET and SEM analysis where the both catalysts showed specific surface areas amounting to 61.33 m^2/g and 71.33 m^2/g respectively.

In the application of these synthesised catalysts for biodiesel synthesis, catalyst B has shown better reactivity with a yield of 88.92% as against a yield of 77.76% obtained with catalyst A. The synthesised FAME has shown great conformity with ASTM D6751 standard.

The synthesised plantain peels potassium hydroxide (KOH) supported rice husk catalyst has shown a tremendous advantage in the commercialisation of biodiesel production in terms of its reusability, recyclability and regeneration ability.

There was a recorded of FFA value in the excess of 5.89% in the raw Castor seed oil which was reduced to 0.78% after esterification reaction before subjecting the oil to transesterification reactions that yielded quality FAME.

In the kinetic study, the experimental data showed great conformity with the rate law and rate constant of the pseudo first order reaction. This goes a long way to show that the trans-esterification of castor oil to fatty acid methyl ester using synthesised plantain peels potassium hydroxide (KOH) doped on rice husk, provided the castor seed oil to methanol molar ratio is kept constant in excess, is a first order reaction. The activation energy of the transesterification reaction was found to be very high which could be attributed to the high viscosity and high fatty acid profile of castor seed oil.

5.2 Recommendations

The challenge of non-renewability of homogeneous catalysts, its non-usability property, the high cost and unavailability of conventional resources, the difficulty of separating homogenous catalysts after reaction, the high amount of wastes after reaction, and the air pollution leading to increased environmental concern has hindered the industrialization of biodiesel which has led to the search for the realization of a biomass based heterogeneous catalyst with high catalytic property and this gap has been closed by the synthesis of ripe plantain peels potassium hydroxide (KOH) doped on rice husk ash.

Hence, following are the recommendations with respect to this work:

The catalyst impregnation ratio should be optimized and synthesised ripe plantain peels potassium hydroxide (KOH) doped on rice husk ash catalyst should be commercialized for biodiesel production.

5.3 Contribution to Knowledge

An active catalyst has been produced from agricultural wastes (potassium hydroxide from plantain peels doped on rice husk) with a specific surface area of 71.33 m^2/g and pore size distribution at 40-100 um of 54.20 micron. The synthesised catalyst on application for biodiesel production gave biodiesel yield of 88.92 % with specific gravity of 0.956, 0.33 % moisture and acid value of 1.374 mgKOH/g. The study further revealed that the transesterification reaction was a pseudo-first order reaction with an activation energy of 36.03 KJ/mol.

REFERENCES

Adokiye, T., Gunorubon, A.J. & Kenkugile, D.K. (2020). Modeling and control of a biodiesel transesterification reactor. *Advances in Chemical Engineering and Science*, 10, 210-224. https://doi.org/10.4236/aces.2020.103016.

Ahmed, F., Giwa, S. O., Ibrahim, M., & Giwa, A. (2016). Production of biodiesel from jatropha curcas seed oil using base catalysed transesterification. *International Journal of ChemTech Research*, Vol.9, No.06 pp 322-332.

Akpan, U. G., Jimoh, A., & Mohammed, A. D. (2006). Extraction, characterisation and modification of castor seed oil. *Leonardo Journal of Sciences*, ISSN 1583-0233 Issue 8, pp. 43-52.

Alueshima, B. M., Eterigho, E. J., & Omale, D. F. (2018). Synthesis of alumina-supported chicken eggshell catalyst for trans-esterification of waste cooking oil. *Earth and Environmental Science* 173 (2018) 012041 doi:10.1088/1755-1315/173/1/012041.

Amin, T. & Amin, N. A. S. (2015). Single and two-step homogeneous catalyzed transesterification of waste cooking oil: optimization by response surface methodology. *International Journal of Green Energy*, 12:9, 888-899, DOI:10.1080/15435075.2014.884501.

Arawande, J. O., & Akinnusotu, A. (2018). Comparative study on extraction and characterisation of castor seed and oil from three different state capitals in Nigeria. *American Journal of Food Science and Nutrition*, ISSN: 2375-3935, Vol. 5 N0. 2, pp. 37-42.

Beruk, A. B., Abel, W. O., Assefa, A. T., & Sintayehu, S. H. (2018). Studies on Ethiopian castor seed (Ricinus communis L.): extraction and characterisation of seed oil. *Journal of Natural Production Resource*, 4(2), 188-190. http://dx.doi.org/10.30799/jnpr.064.18040204.

Chandrasekhar, S., Pramada, P. N., & Majeed, J. (2006). Effect of calcination temperature and heating rate on the optical properties and reactivity of rice husk ash. *Journal of Materials Science*, 41(23), 7926–7933. doi:10.1007/s10853-006-0859-0

Chen, K. T., Wang, J. X., Dai, Y. M., Wang, P. H., Liou, C. Y., Nien, C. W. & Chen, C. C. (2013). Rice husk ash as a catalyst precursor for biodiesel production. *Journal of the Taiwan Institute of Chemical Engineers*, 44(4), 622–629. doi:10.1016/j.jtice.2013.01.006.

Dhikrah, I., SM, Dangoggo, NA, Sani, AS, Baki , BU, B., & MS, J. (2018). Optimization of biodiesel production from jatropha seed oil, using sulphated zirconia as catalyst. *Chemical Sciences Journal*, 09(02). doi:10.4172/2150-3494.1000184.

Efeovbokhan, V. E., Omoleye, J. A., & Kalu, E. E. (2016). Extraction and use of potassium hydroxide from ripe plantain peels ash for biodiesel production. *Journal of Biobased Materials and Bioenergy*, Vol. 10, No. 1, pp 1–9.

Efeovbokhan, V. E., Omoleye, J. A., Kalu, E. E. & Udonne, J. D. (2017). Kinetics of base catalysed trans-esterification of jatropha oil using potassium hydroxide extract from ripe plantain peels. *International Journal of Applied Engineering* Research ISSN 0973-4562 Volume 12, Number 14 pp. 4539-4548.

Etim, A., Betiku, E., Ajala, S., Olaniyi, P., & Ojumu, T. (2018). Potential of ripe plantain fruit peels as an ecofriendly catalyst for biodiesel synthesis: optimization by artificial neural network integrated with genetic algorithm. Sustainability, 10(3), 707. doi:10.3390/su10030707

FAOSTAT. Statistical databases. food and agriculture organization of the United Nations. Statistics Division. 2019. Available online: www.fao.org/faostat/en/#data/QC (accessed on 17 July 2021).

Feng, G. & Zhen F. (2016). Biodiesel production with solid catalysts. *Chinese Academy of Sciences, Biomass Group, Xishuangbanna Tropical Botanical Garden, China.*

Gad-Elkareem, M. A., Abdelgadir, E. H., Badawy, O. M., & Kadri, A. (2019). Potential antidiabetic effect of ethanolic and aqueous-ethanolic extracts of Ricinus communis leaves on streptozotocin-induced diabetes in rats. PeerJ, 7, e6441. http://dx.doi.org/10.7717/peerj.6441. PMid:30805250.

Gashaw, A., Getachew, T. & Teshita, A. (2015). A review on biodiesel production as alternative fuel. *Journal of forest products & industries*, 4(2), 80 – 85.

Gebremariam, S.N. & Marchetti, J.M. (2017). Biodiesel production technologies: review. *Journal of Energy*, 5(3), 425 – 457.

Hossain, M. N., Bhuyan, M. S. U. S., Alam, A. H. M. A., & Seo, Y. C. (2018). Biodiesel from hydrolyzed waste cooking oil using a S-ZrO2/SBA-15 super acid catalyst under sub-critical conditions. Energies Journal. 11, 299; doi:10.3390/en11020299.

Keera, S. T., El Sabagh, S. M., & Taman, A. R. (2018). Castor oil biodiesel production and optimization. *Egyptian Journal of Petroleum* 27, 979–984.

Lani, N. S., Ngadi, N., Yahya, N. Y., & Rahman, R. A. (2017). Synthesis, characterisation and performance of silica impregnated calcium oxide as heterogeneous catalyst in biodiesel production. Journal Clean Production 146, 116–124.

Ling Zhou (2013). Reaction kinetics of biodiesel production by using low quality feedstock. Masters' thesis, University of Regina.

Maniam, G. P., Hindryawati, N., & Yusoff, M. M. (2015). Rice husk silica supported oil palm fruit ash as a catalyst in the transesterification of waste frying oil. *Journal of Engineering and Technology*, Vol. 6 No.1 January-June 2015.

Marwaha, A., Dhir, A., Mahla, S. K., & Mohapatra, S. K. (2018). An overview of solid base heterogeneous catalysts for biodiesel production. *Catalysis Reviews*, 60(4), 594–628. doi:10.1080/01614940.2018.1494782.

Mishra, V. K., & Goswami, R. (2017). A review of production, properties and advantages of biodiesel. Biofuels, 9(2), 273–289. doi:10.1080/17597269.2017.1336350.

Mubofu, E. B. (2016). Castor oil as a potential renewable resource for the production of functional materials. Sustainable Chemical Processes, 4(1), 11. http://dx.doi.org/10.1186/s40508-016-0055-8.

Mujeeb, M. A., Vedamurthy, A. B. & Shivasharana, C.T. (2016). Current strategies and prospects of biodiesel production: A review. *Advances in Applied Science Research* 7(1) 120 – 133.

Muniandy, L., Adama, F., Mohamed, A. R., & Eng-Poh, N. (2014). The synthesis and characterisation of high purity mixed microporous/mesoporous activated carbon from rice husk using chemical activation with NaOH and KOH. *Microporous and Mesoporous Materials 197, 316–323.*

Naik, B. (2018). Botanical descriptions of castor bean the castor bean genome (pp. 1-14). Switzerland: Springer.

Nasreen, S., Nafees, M., Qureshi, L. A., Asad, M. S., Sadiq, A., & Ali, S. D. (2018). Review of catalytic transesterification methods for biodiesel production. *Biofuels - State of Development*. doi:10.5772/intechopen.75534.

Nhung, D., Trinh, N., Tuan, D. P., Tran, H., Dang, P., & Nguyen, H. (2018). Synthesis of silica nanoparticles from rice husk ash. Science and Technology Development Journal. 20. 50-54. 10.32508/stdj.v20iK7.1211.

Nisar, S., Ishaq, A., Sultana, A., Faiza, & Shehzad, R. M. (2017). Reactions other than transesterification for biodiesel production. *International Journal of Chemical and Biochemical Sciences*. 12(2017):141-146.

Nurdin, S., Rosnan, N.A., Ghazali, N.S., Gimbun, J., Nour, A.H. & Haron, S.F., (2015). Economical biodiesel fuel synthesis from castor oil using mussel shell base (MC – BS). *International Conference on Alternative Energy in Developing Countries and Emerging Economies.*79 (2015), 576 – 587.

Olabanji, I. O., Oluyemi, E. A., & Solomon O. A. (2012). Metal analyses of ash derived alkalis from banana and plantain peels (*Musa spp*.) in soap making. *African Journal of Biotechnology* Vol. 11(99), pp. 16512-16518.

Oladipo, B., Ojumu, T., & Betiku, E. (2018). Potential of pawpaw peels as a base heterogeneous catalyst for biodiesel production: Modeling and optimization studies.

Panhwar, T., Mahesar, S. A., Mahesar, A. W., Kandhro, A. A., Talpur, F. N., Laghari, Z. H., Chang, A. S., & Hussain Sherazi, S. T. (2016). Characteristics and composition of a high oil yielding castor variety from Pakistan. *Journal of Oleo Science*, 65(6), 471-476. http://dx.doi.org/10.5650/jos.ess15208. PMid:27250560.

Sarve, A., Varma, M. N., & Sonawane, S. S. (2015). Optimization and kinetic studies on biodiesel production from Kusum (Schleichera triguga) oil using Response Surface Methodology. Journal of Oleo Science, 64(9), 987–997. doi:10.5650/jos.ess15069.

Saydut, A., Kafadar, A. B., Aydin, F., Erdogan, S., Kaya, C., & Hamamci, C. (2016). Effect of homogeneous alkaline catalyst type on biodiesel production from soybean [Glycine max (L.) Merrill] oil. *Indian Journal of Biotechnology*, Vol.15, pp 596-600.

Sbihi, H. M., Nehdi, I. A., Mokbli, S., Romdhani-Younes, M., & Al-Resayes, S. I. (2018). Hexane and ethanol extracted seed oils and leaf essential compositions from two castor plant (Ricinus communis L.) varieties. Industrial Crops and Products, 122, 174-181. http://dx.doi.org/10.1016/j.indcrop.2018.05.072.

Soltani, N., Bahrami, A., Pech-Canul, M. I., & Gonzàlez, L.A. (2015). Review on the physicochemical treatments of rice husk for production of advanced materials. *Chemical Engineering Journal*. 264, 899–935.

Thabet, A., Basheer, C., Maung, T. H., Al-Muallem, H. A., & Kalanthoden, A. N. (2015). Rice husk supported catalysts for degradation of chlorobenzenes in capillary microreactor. *Journal of Nanomaterials*, 2015, 1–9. doi:10.1155/2015/912036

Touhami, D., Zhu, Z., Balan, W. S., Janaun, J., Haywood, S., & Zein S. (2017). Characterisation of rice husk-based catalyst prepared via conventional and microwave carbonisation. *Journal of Environmental Chemical Engineering*. 5, 2388–2394. DOI: 10.1016/j.jece.2017.04.020.

Usman, Y. O., Omoniyi, K. I., Nwokem, N. C., Maikano, S. A. & Nwokem, C. O. (2018). Comparative study of the yield of reducing sugar from hydrolysis of *Ximenia caffra* seed coat and *Phoenix dactylifera* stone using bioalkali extracted from plantain peel. *Tropical Journal of Natural Product Research*, 2(4):162-166. doi.org/10.26538/tjnpr/v2i4.2.

Yacob, A.R., Mohmedahmed, A.M., Azam bin, M.A. & Zaki, M. (2017). Acid modified jourdiqua clay for methanolysis of castor oil. *Journal of Pharmacovigilance*, 5(5), 1 – 5. DOI: 10.4172/2329-6887.1000240.

Yeboah, A., Ying, S., Lu, J., Xie, Y., Amoanimaa-Dede, H., Boateng, K. G. A., Chen, M. & Yin, X. (2020). Castor oil (*Ricinus communis*): a review on the chemical

composition and physicochemical properties. *Food Science and Technology*, ISSN 1678-457X, DOI: https://doi.org/10.1590/fst.19620

Ying, S., Hill, A. T., Pyc, M., Anderson, E. M., Snedden, W. A., Mullen, R. T., She, Y. M., & Plaxton, W. C. (2017). Regulatory phosphorylation of bacterial-type PEP carboxylase by the Ca2+-dependent protein kinase RcCDPK1 in developing castor oil seeds. Plant Physiology, 174(2), 1012-1027. http://dx.doi.org/10.1104/pp.17.00288. PMid:28363991.

Yusuf, A., Mamza, P., Ahmed, A., & Agunwa, U. (2015). Extraction and characterisation of castor seed oil from wild Ricinus communis Linn. International *Journal of Science, Environment and Technology*, 4(5), 1392-1404.

Zahan, K., & Kano, M. (2018). Biodiesel production from palm oil, its by-products, and mill effluent: A Review. Energies, 11(8), 2132. doi:10.3390/en11082132.

APPENDICES

APPENDIX A

Calculations on Castor Oil Characterisation

Specific gravity

The weight of an empty specific gravity bottle of volume 10 ml was determined and recorded as M_0. The empty specific gravity bottle was then filled with water and the weight re-determined as M_2. The bottled was then emptied, washed, dried and refilled with the castor seed oil and the weight recorded as M_1.

Volume of fluid in the bottle = 10 ml

Mass of empty specific gravity bottle, M_0 = 23.113g

Mass of empty specific gravity bottle + water, M_2 = 51.216g

Mass of empty specific gravity bottle + castor seed oil, M_1 = 49.952g

The specific gravity of the castor seed oil = $\frac{M_1 - M_0}{M_2 - M_0}$ $\frac{49.752 - 23.113}{51.216 - 23.113} = \frac{26.639}{28.103} = 0.948$

Determination of peroxide value

1000 = constant for peroxide value,

Titre Value of sodium thiosulphate for blank test = 13.42 ml

Titre Value of sodium thiosulphate for the oil sample = 9.13 ml

Normality of the standard sodium thiosulphate = 0.002M

Weight of the oil used = 1 g.

Peroxide value, $PV = \frac{(T_1 - T_2)\ x\ M\ x\ 1000}{W} = PV = \frac{(13.42 - 9.13)\ x\ 0.002\ x\ 1000}{1}$

PV = (13.42 – 9.13) x 0.002 x 1000 = 8.58 mgKOH/g

Determination of iodine value

Mass of oil sample used, M = 5g

Volume of sodium thiosulphate used for the oil sample, V_2 = 13.80 ml

Volume of sodium thiosulphate used for blank test, V_1 = 48.40 ml

Normality of sodium thiosulphate used, N = 0.1N

Iodine Value, $IV = \frac{126.9 \text{ x N x } (V_1 - V_2)\ x\ 100}{M} = \frac{126.9 \text{ x } 0.1 \text{ x } (48.40 - 13.80)}{5} = \frac{126.9 \text{ x } 0.1 \text{ x } 34.60}{5} = \frac{439.074}{5}$

= 87.815 g I_2/100 oil

Moisture content

Original weight of the sample before drying, W_1 = 40.00 g

Weight of the sample after drying, W_2 = 38.75 g

Moisture $= \frac{40 - 38.75}{38.75}\ x\ 100\% = \frac{1.25}{38.75}\ x\ 100\%$ = 3.23%

Acid value

1g of oil was weighed into a mixture of 25 ml of diethyl ether, 25ml of alcohol and 4 drops of phenolphthalein in a 250cm^3 conical flask. The solution was titrated using 0.1M NaOH until a persistent colour appeared.

Acid value $= \frac{V_o \text{ x N x } 56.10}{W_o}$

Weight of oil used, W_0 = 1g

Volume of NaOH used:

1st titre value = 1.95ml

2nd titre value = 2.15ml

Average titre value, $V_0 = \frac{2.25 + 1.95}{2} = \frac{4.20}{2}$ = 2.10ml

Normality of NaOH used, N = 0.1M

Acid value = $\frac{56.1\times0.1\times2.10}{1}$ = 11.78 mgKOH/g

Free fatty acid

Free fatty acid is the acid value expressed in percentage.

FFA = $\frac{acid\ value}{2}$ = $\frac{11.78}{2}$ = 5.89%

Esterification of castor oil

Esterification was done to reduce the FFA content of the oil to limit saponification process.

Weight of oil used, W_0 = 3g

Volume of NaOH used:

1st titre value = 0.83 ml

2nd titre value = 0.84 ml

Average titre value, V_0 = $\frac{0.83+0.84}{2}$ = $\frac{1.67}{2}$ = 0.835 ml

Normality of NaOH used, N = 0.1M

Acid value = $\frac{56.1\ x\ 0.1\ x\ 0.835}{3}$ = $\frac{4.68435}{3}$ = 1.56 mgKOH/g

FFA = $\frac{acid\ value}{2}$ = $\frac{1.56}{2}$ = 0.78%

Calculations on the Stoichiometry of Transesterification Reaction

Sample calculation:

The specific gravity of castor seed oil = 0.948

Volume of oil used = 15ml

Weight of oil used:

1ml of oil = 0.948

15ml of oil = ?

0.948 x 15ml = 14.22 g of oil

Oil to methanol molar ratio of 1:6

14.22 g of oil x 6 = 85.32 g

85.32 g of methanol

Specific gravity of methanol = 0.791

Therefore, for the transesterification reaction, the volume of methanol required = mass of methanol/specific gravity of methanol

= 85.32/0.791

= 107.86 ml

APPENDIX B

The Result Obtained from Response Surface Methodology for the Biodiesel Production

Table B1: Predicted vs Actual yields of biodiesel for catalysts A and B

Run	Weight of FAME produced using Catalyst A (g)	FAME yield of catalyst A (%)	Weight of FAME produced using Catalyst B (g)	FAME yield of catalyst B (%)
1	9.890	69.55	11.369	79.95
2	10.914	76.75	12.511	87.98
3	8.007	56.31	9.311	65.48
4	9.213	64.79	10.691	75.18
5	8.990	63.22	9.786	68.82
6	9.634	67.75	11.154	78.44
7	9.213	64.79	10.691	75.18
8	9.334	65.64	10.364	72.88
9	8.622	60.63	10.142	71.32
10	7.869	55.34	8.913	62.68
11	9.613	67.6	10.782	75.82
12	7.869	55.34	8.913	62.68
13	8.334	58.61	9.985	70.22
14	7.797	54.83	9.239	64.97
15	7.512	52.83	8.684	61.07
16	10.914	76.75	12.511	87.98
17	11.057	77.76	12.644	88.92
18	9.634	67.75	11.154	78.44
19	9.803	68.94	11.517	80.99
20	7.652	53.81	8.956	62.98

Determination of Percentage Yield of Fatty Acid Methyl Ester

Percentage yield = (Weight of FAME produced/ Weight of castor seed oil used) x 100%

Sample calculation:

For run 1, catalyst A,

Weight of FAME produced = 9.890 g

Weight of castor seed oil used = 14.22 g

%Yield = (9.89/14.22) x 100% = 0.6955 x 100% = 69.55%

The Result of the Kinetic Study of the Transesterification of Castor Seed Oil

Table B2: The weight of biodiesel produced at varying time with catalyst loading of 3.0 wt/wt%, methanol-to-oil molar ratio of 6:1 & temperatures of 60 ^{o}C, 61 ^{o}C and 62 ^{o}C

Time (hrs)	Weight of biodiesel (g)	Weight of biodiesel (g)	Weight of biodiesel (g)
t_f	Temperature of 60 ^{o}C	Temperature of 61 ^{o}C	Temperature of 62 ^{o}C
0.5	8.855	7.45	5.925
1.0	11.864	11.176	11.103
1.5	12.118	11.91	11.453
2.0	13.289	12.824	12.580

Determination of castor oil conversion

Conversion, X_{Af} = Weight of FAME produced/ Weight of castor seed oil used

Sample calculation:

For 0.5 hrs time, temperature of 60^{o}C,

Weight of FAME produced = 8.855 g

Weight of castor seed oil used = 14.22 g

Conversion, X_{Af} = 8.855/14.22 = 0.6227

Table B3: The conversions obtained from the experimental data

Time (hrs)	**Conversion, X_{Af}**		
t_f	**Temperature of 60 ^{o}C**	**Temperature of 61 ^{o}C**	**Temperature of 62 ^{o}C**
0.5	0.6227	0.5239	0.4167
1.0	0.8543	0.7859	0.7808
1.5	0.8722	0.8376	0.8054
2.0	0.9345	0.9018	0.8847

Calculation of the Characterisation of the Fatty Acid Methyl Ester

Specific gravity

Volume of fluid in the bottle = 10 ml

Mass of empty specific gravity bottle, M_0 = 23.113g

Mass of empty specific gravity bottle + water, M_2 = 75.106 g

Mass of empty specific gravity bottle + FAME, M_1 = 72.221 g

Specific gravity = $\frac{M_1 - M_0}{M_2 - M_0} = \frac{49.712 - 23.113}{50.934 - 23.113} = \frac{26.599}{27.821}$ = 0.956

Moisture content

Volume of oil sample = 4ml

Weight of empty dish = 14.243g

Weight of dish + weight of wet FAME, W_1 = 18.067g

Weight of dish + weight of dry FAME, W_2 = 18.007g

Moisture content = $\frac{W_1 - W_2}{W_2} \times 100\% = \frac{18.067 - 18.007}{18.067} \times 100\% = \frac{0.06}{18.067} \times 100\% = 0.33\%$

Acid value

Mass of oil sample, M_1 = 5g

1st titre value = 1.10cm^3

2nd titre value = 1.05cm^3

Average titre value, V = 1.08cm^3

Normality of NaOH, N = 0.1N

Acid value = $\frac{56.1 \times 1.08 \times 0.1}{5} = 1.21$

Acid value $= \frac{V_o \text{ x N x } 56.10}{W_o}$

Weight of oil used, W_0 = 5g

Volume of NaOH used:

1st titre value = 1.25ml

2nd titre value = 1.20ml

Average titre value, V_0 = $\frac{1.25+1.20}{2} = \frac{2.45}{2}$ = 1.225 ml

Normality of NaOH used, N = 0.1M

Acid value = $\frac{56.1 \times 0.1 \times 1.225}{5} = \frac{6.87}{5}$ = 1.374 mgKOH/g

Free fatty acid

Free fatty acid is the acid value expressed in percentage.

$$\%FFA = \frac{acid\ value}{2} = \frac{1.374}{2} = 0.687\%$$

Determination of catalyst recyclability

Table B4: Experimental data for recyclability yield

Number of Cycle	FAME yield (g)
1	12.644
2	12.572
3	12.498
4	12.251

Table B5: Calculated data for recyclability yield

Number of Cycle	% FAME yield (%)
1	88.92
2	88.41
3	87.89
4	86.15